General Disclaimer

One or more of the Following Statements may affect this Document

- This document has been reproduced from the best copy furnished by the organizational source. It is being released in the interest of making available as much information as possible.

- This document may contain data, which exceeds the sheet parameters. It was furnished in this condition by the organizational source and is the best copy available.

- This document may contain tone-on-tone or color graphs, charts and/or pictures, which have been reproduced in black and white.

- This document is paginated as submitted by the original source.

- Portions of this document are not fully legible due to the historical nature of some of the material. However, it is the best reproduction available from the original submission.

Produced by the NASA Center for Aerospace Information (CASI)

(NASA-CR-159413) CTS TEP THERMAL ANOMALIES: HEAT PIPE SYSTEM PERFORMANCE Final Report (TRW Defense and Space Systems Group) 61 p HC A04/MF A01 CSCL 20D

N78-29410

Unclas
G3/34 29172

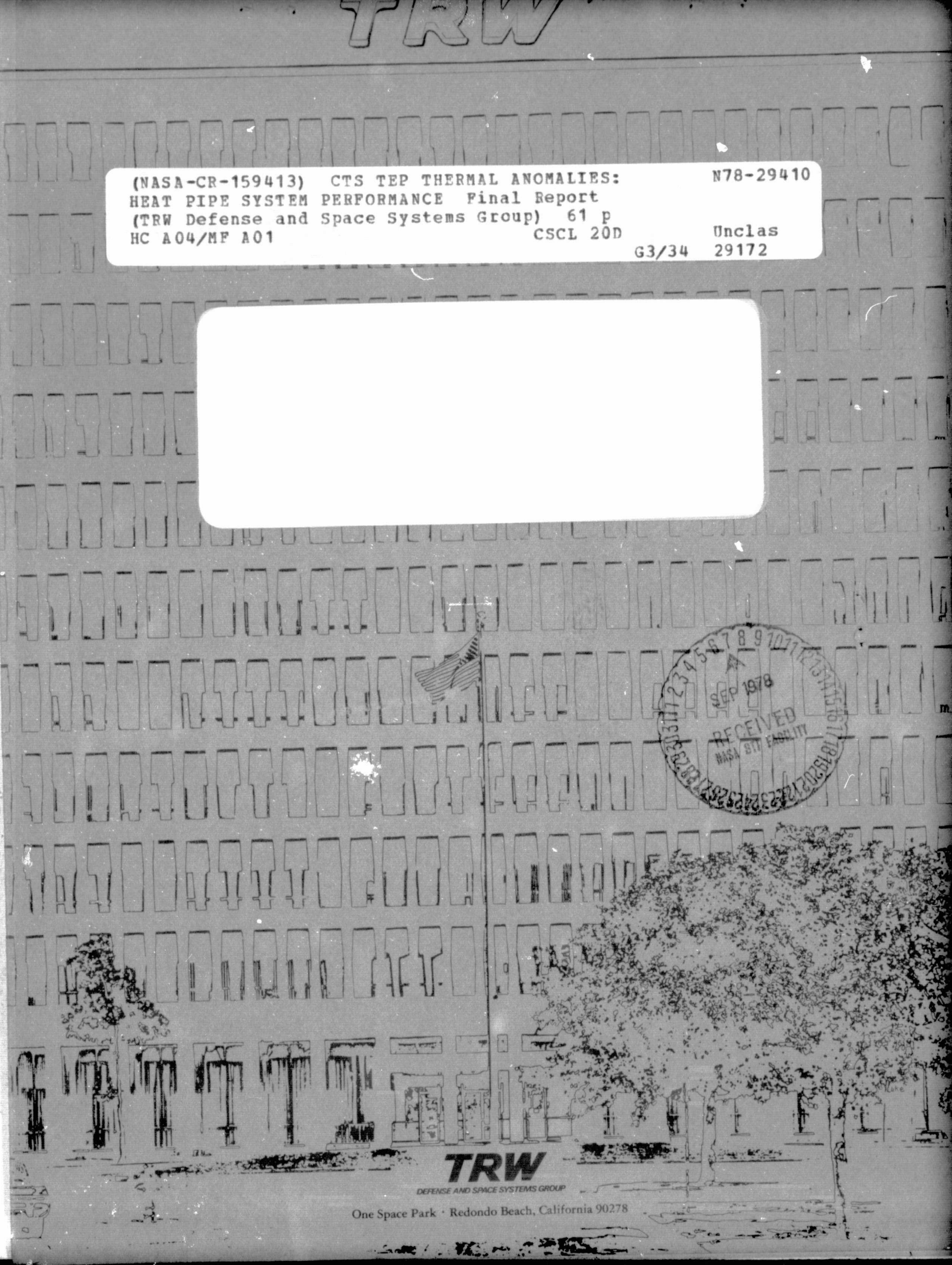

SEP 1978
RECEIVED
NASA STI FACILITY

TRW

DEFENSE AND SPACE SYSTEMS GROUP

One Space Park · Redondo Beach, California 90278

CTS TEP THERMAL ANOMALIES –

HEAT PIPE SYSTEM PERFORMANCE

B.D. MARCUS

30 NOVEMBER 1977

Prepared under Contract NAS3-21012
for NASA Lewis Research Center

TRW Sales No. 32458.000

TRW
DEFENSE AND SPACE SYSTEMS GROUP
ONE SPACE PARK • REDONDO BEACH, CALIFORNIA 90278

CONTENTS

		Page
1.	INTRODUCTION AND SUMMARY	1-1
2.	OBSERVED ANOMALOUS BEHAVIOR	2-1
	2.1 Occurrences	2-1
	2.2 Characteristics	2-1
	2.3 Anomalies Associated with Eclipse Seasons	2-8
3.	CONSISTENCY OF ANOMALOUS BEHAVIOR WITH HEAT PIPE OPERATING CHARACTERISTICS	3-1
	3.1 Heat Pipe Capacity	3-1
	3.2 Heat Pipe Thermal Resistance	3-5
	3.3 Heat Pipe Vapor Temperature	3-6
	3.4 Condenser Freezing Under Load	3-7
	3.5 Flight Experiments Mostly Consistent with Open Artery Operation	3-10
	3.6 Hypothetical Performance Model	3-12
4.	ARTERY DEPRIMING MECHANISMS	4-1
	4.1 Condenser Freezing	4-2
	4.2 Marangoni Flow	4-3
	4.3 Gas Evolution Within Arteries	4-4
	4.3.1 Nucleation Experiment	4-6
	4.4 Summary	4-7
5.	REFERENCES	5-1
APPENDIX A	THERMAL RESISTANCE CALCULATIONS	A-1
APPENDIX B	TRANSIENT THERMAL ANALYSIS OF ANOMALIES	B-1
APPENDIX C	EXPERIMENT PROTOCOL FOR FLIGHT TESTING OF CTS HEAT PIPES	C-1
APPENDIX D	PRIMING STUDIES WITH A GLASS HEAT PIPE	D-1

1. INTRODUCTION AND SUMMARY

The Communications Technology Satellite (CTS) was launched in January 1976 and is now approaching completion of two years of operation. The major payload on the CTS is the Transmitter Experiment Package (TEP) - a high power traveling wave tube transmitter and associated power processing equipment. Temperature control of the traveling wave tube is provided primarily by a variable conductance heat pipe (VCHP)/Radiator system which transports and rejects most of the heat dissipated in the tube body. Figure 1 shows the VCHP/Radiator System and the six positions at which temperatures are measured in flight.

On four occasions in 1977, the TEP has recorded thermal anomalies wherein the tube body experienced an unanticipated increase in temperature which continued until the operating power was decreased. However, except for these anomalous periods, the TEP operated normally with no permanent changes in thermal characteristics.

TRW has participated in a coordinated effort to investigate these thermal anomalies. In particular, our efforts have been directed at evaluating potential heat pipe implication. The VCHP/Radiator System is in the thermal path from the tube body to space and would normally be investigated in an anomalous behavior analysis. However, the heat pipes are particularly suspect in this case. They have arterial wicks and exhibit multiple heat transport capacities - depending on how many arteries are primed. Thus, they provide a potential explanation to the sporadic and fully recoverable nature of the anomalies. Interface failures - the other prime candidate - would not likely recover to pre-failure conditions by temporarily reducing power.

The heat pipe investigation has included analysis of flight data for both normal and anomalous operation, laboratory experiments at both LeRC and TRW, and flight experiments with the CTS. The results of this investigation are not thoroughly conclusive but do suggest that the heat pipes are likely involved. The bulk of the evidence shows that the anomalous behavior is consistent with depriming of the heat pipe arteries. However, no consistent cause of artery depriming has been identified - nor can repriming of the arteries be explained in several cases.

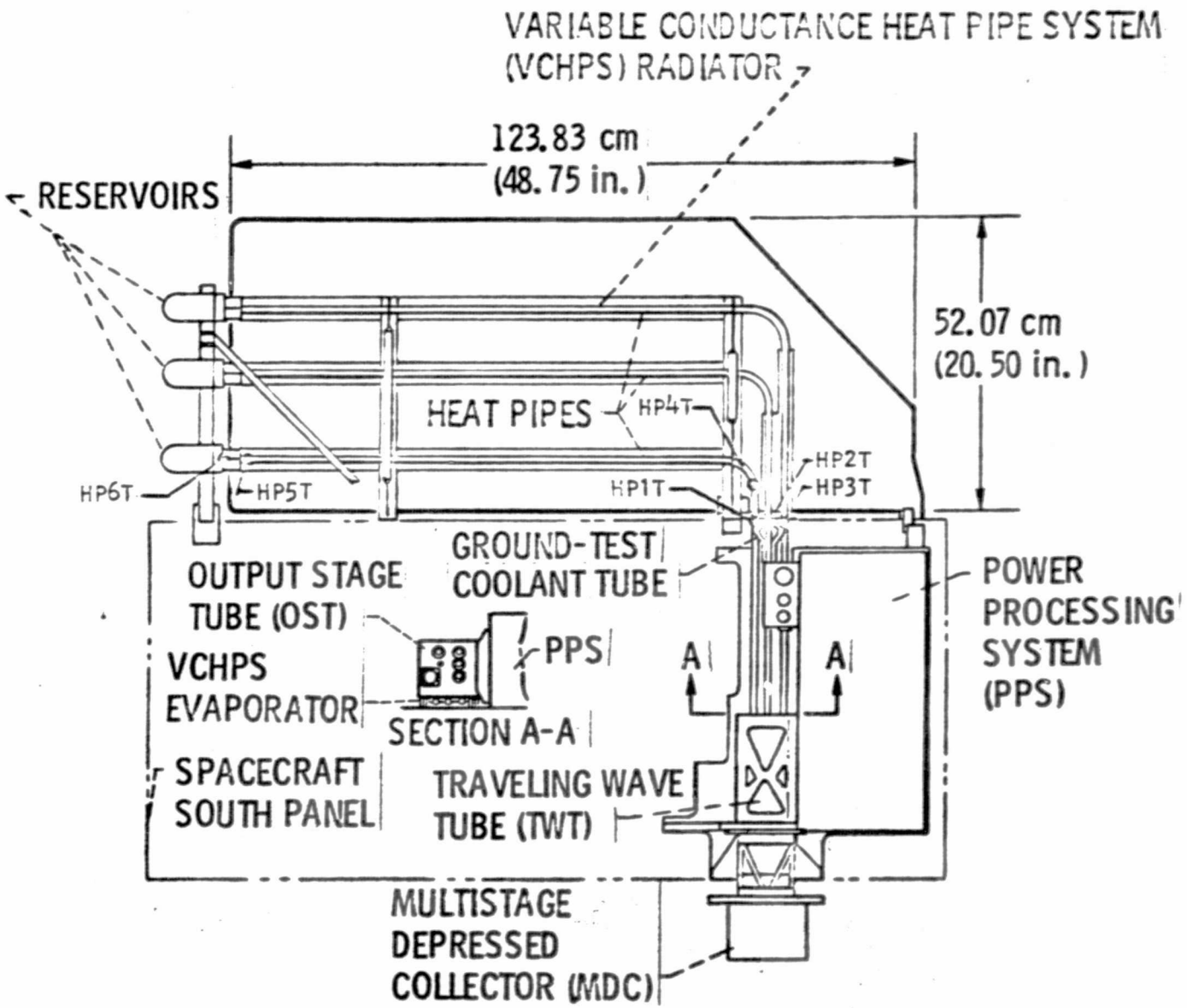

Figure 1. CTS Transmitter Experiment Package

ORIGINAL PAGE
OF POOR QUALITY

PRECEDING PAGE BLANK NOT FILMED

One positive result of the investigation is that the stable operating power (≈130 watts RF output) has been identified for the anomalous mode. Below this level, which only represents a reduction of RF output to about 60 percent of saturation, the system operates in a stable and fail-safe condition.

PRECEDING PAGE BLANK NOT FILMED

2. OBSERVED ANOMALOUS BEHAVIOR

2.1 OCCURRENCES

Four anomalies have been identified through the end of September 1977. Although the CTS has been operational since January 1976, all four anomalies have occurred in 1977. They are listed in Table 1, numbered in order of discovery rather than occurrence to be consistent with prior documentation. Tabulated data includes date, day of year, time, orbital position in degrees and the sun angle to the orbit plane. Figure 2 shows the spacecraft orientation at various orbit positions.

2.2 CHARACTERISTICS

The observed thermal anomalies are characterized by an unanticipated rise in the tube body temperature beyond the normal operating range which continues until the power is reduced. Figure 3 shows the tube body temperature history for each of the four anomalies.

The rate of temperature rise during the excursion is correlated with the power dissipated within the tube body. This can be determined from the RF output as follows:

$$\text{Dissipated Power} = 20 + 0.6136\ RF_{OUT}\ \text{(watts)} \qquad (1)$$

In turn, the RF output is related to the TEPP power, as shown in Figure 4. Combining Equation (1) with Figure 4 permits constructing Figure 5, which relates the dissipated power to the TEP power. Under steady state conditions the dissipated power is all conducted to the tube baseplate. During an anomaly, however, a portion is stored in the various tube components, causing the rise in temperature.

Table 2 lists the power dissipation at the start of each anomaly. Comparing Figure 3 and Table 2 shows that the higher the power dissipation the more rapid the temperature excursion (note that the time scale for anomaly No. 4 is expanded).

Typically, the anomaly begins after sustained operation at essentially constant input power and has no associated change in RF output. Thus, heat dissipation is relatively constant through the anomaly and the rise in tube body temperature must be associated with an increase in thermal resistance between the source and sink. Such a resistance increase could be caused by a

Table 1. Identified Thermal Anomalies

Number	Date	Day of Year	Time (E.S.T.)	Orbit Position (Degrees)	Sun Angle (Degrees)
1	3/16/77	75	14:25	173	-2.0
2	4/11/77	101	13:43	165	+8.1
3	3/23/77	82	13:00	149	+0.8
4	9/10/77	253	09:20	95	

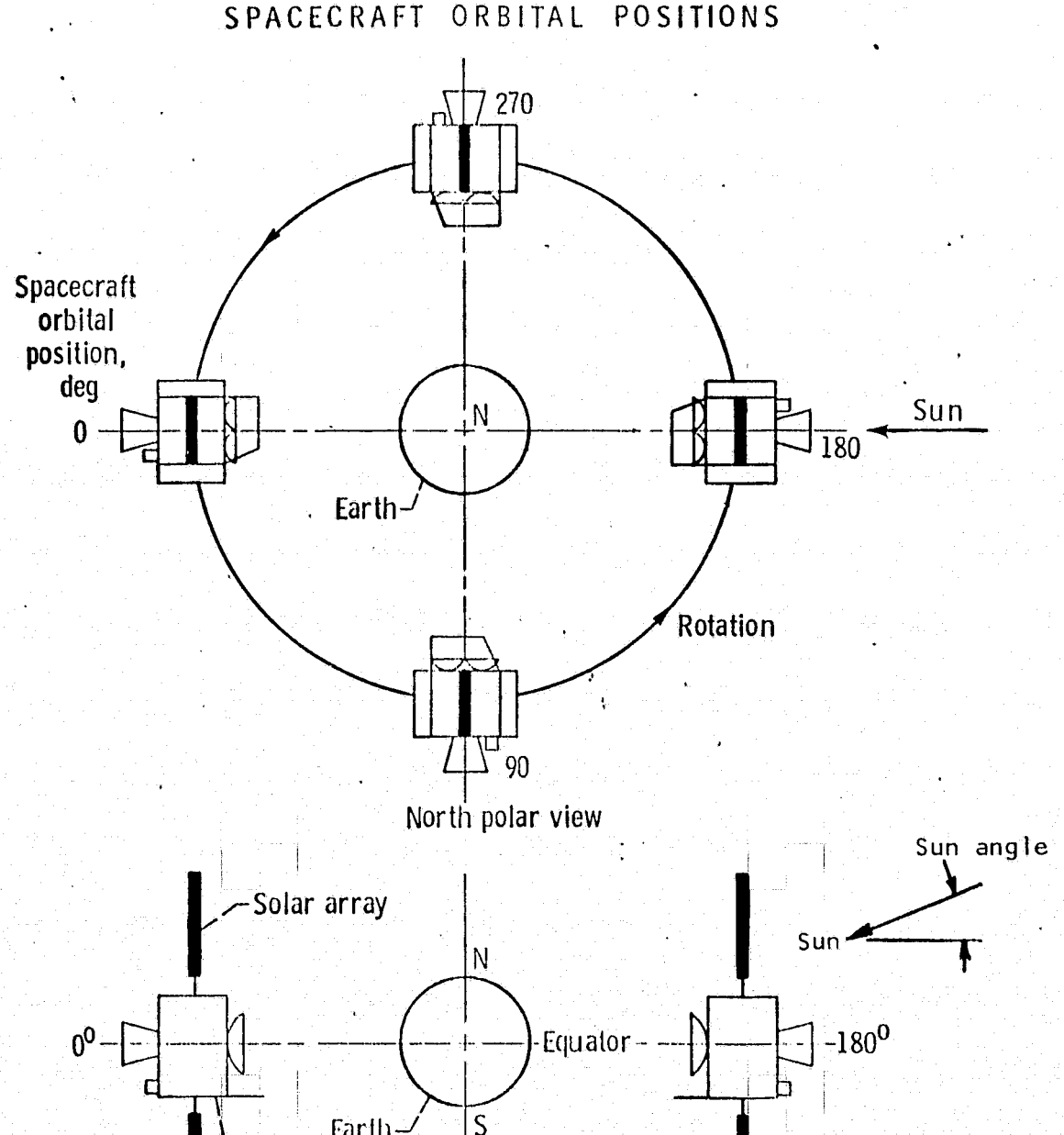

Figure 2. Spacecraft Orientation With Orbital Position

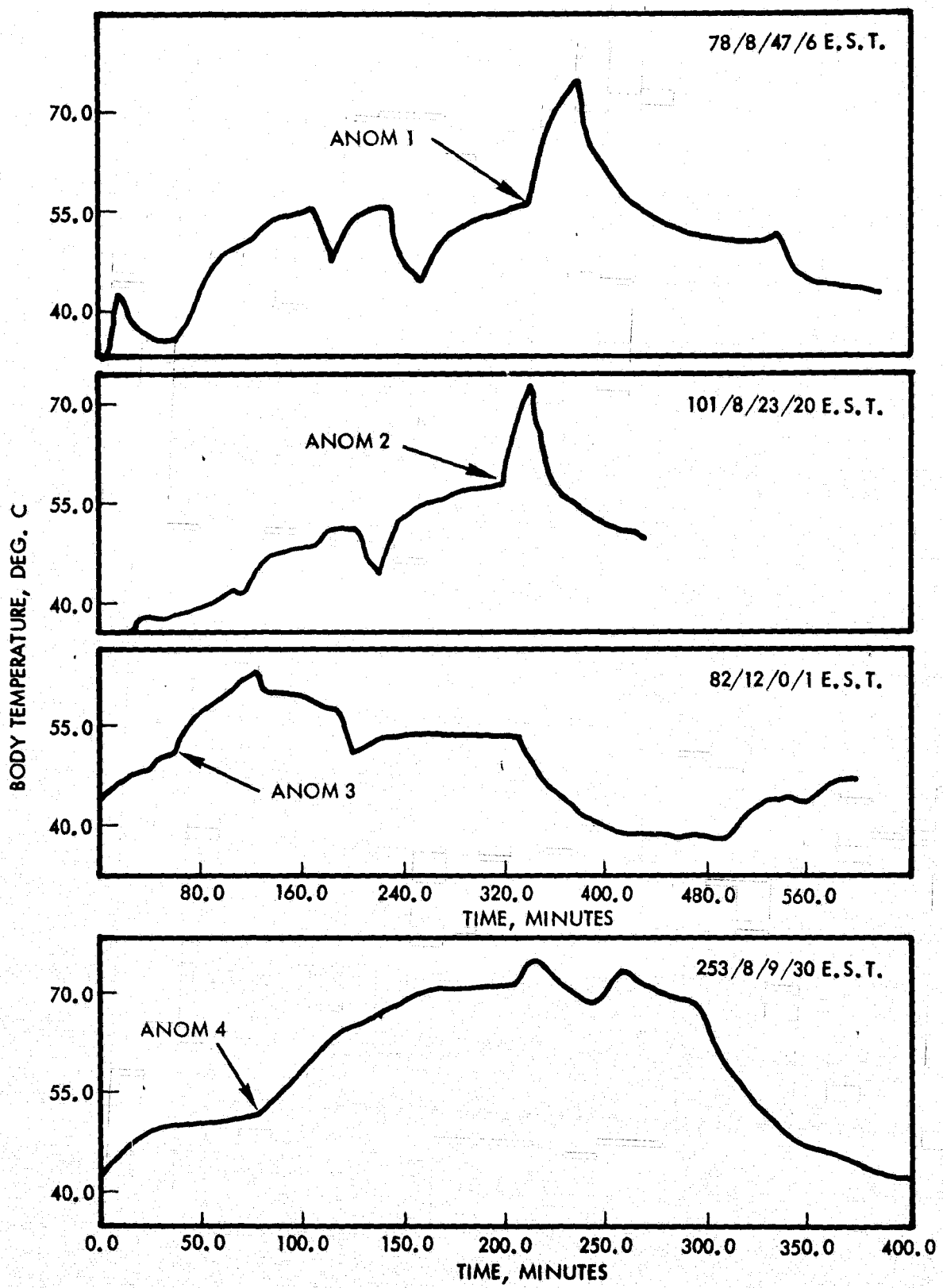

Figure 3. CTS Thermal Anomalies: Tube Body Temperature Versus Time

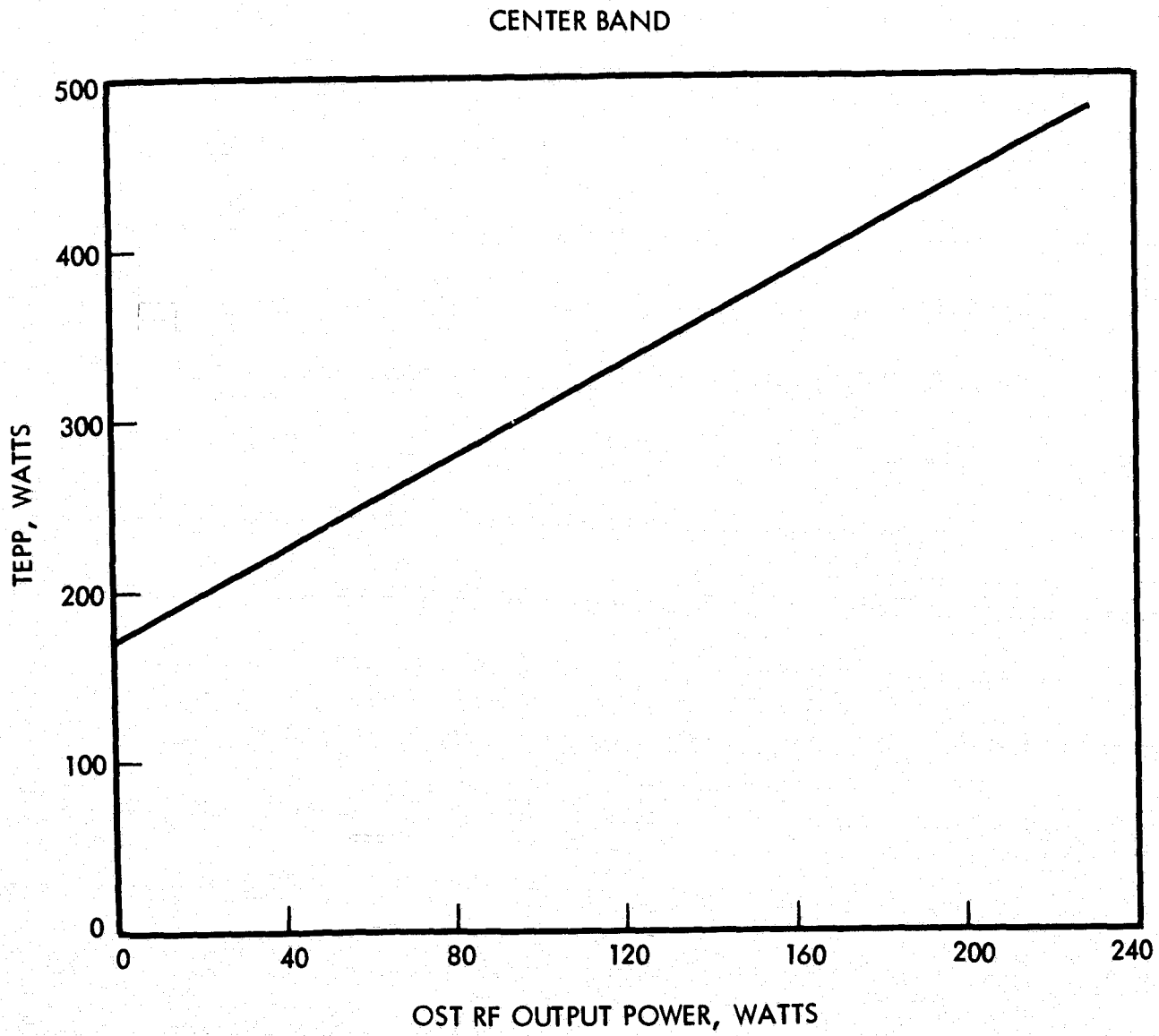

Figure 4. TEP Power Versus OST RF Output

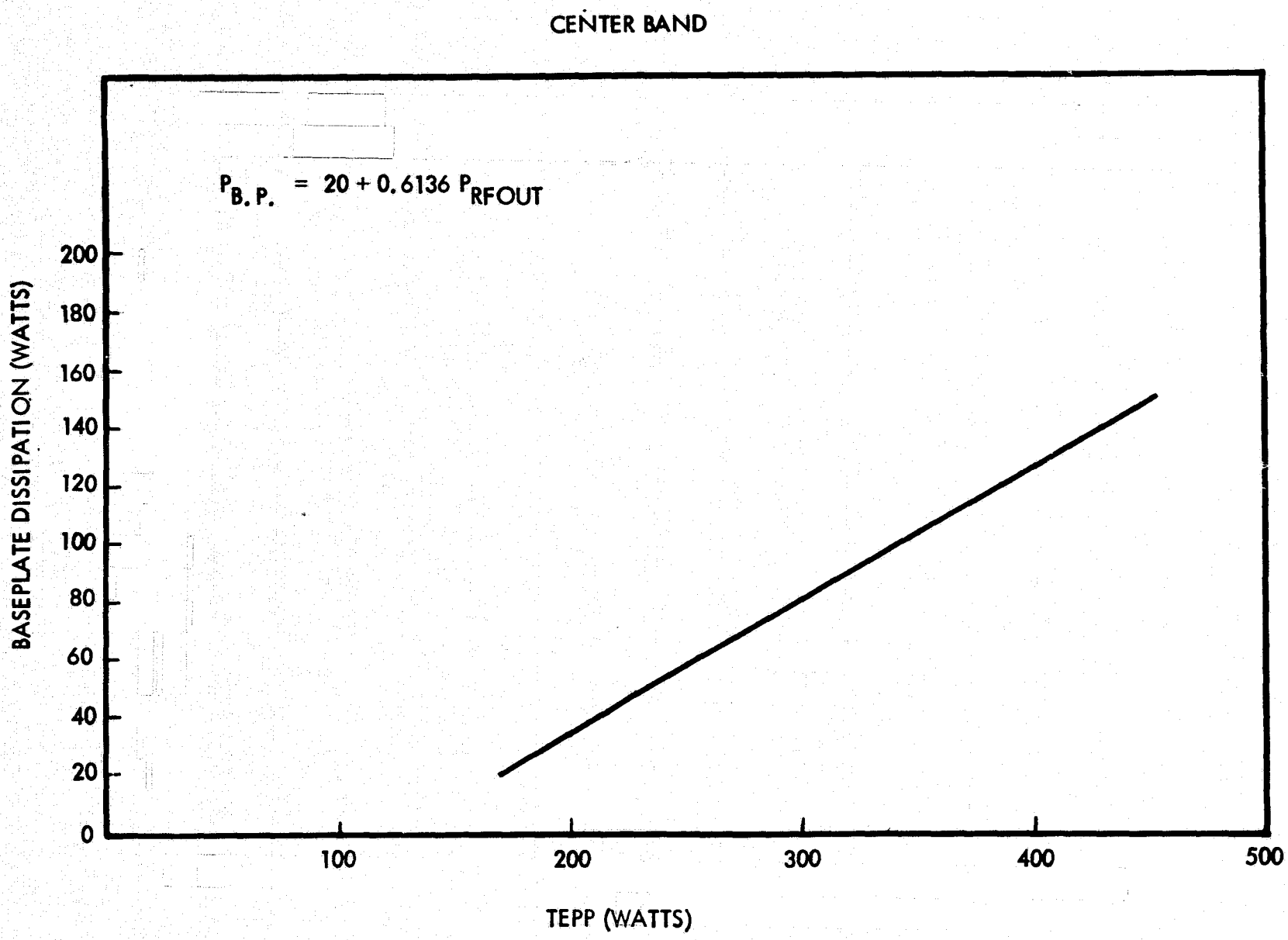

Figure 5. Dissipated Power to Baseplate Versus TEP Power

Table 2. Power Dissipation in Tube Body Prior to and During Anomalies (Watts)

Anomaly	TEP Power	RF Out	Dissipation in Body
1 (Day 75)	435	196	140
2 (Day 101)	450	208	148
3 (Day 82)	395	165	121
4 (Day 253)	440	200	143

degradation in heat pipe performance or any other link in the thermal path. As shown in Figure 6, there are several interfaces (Indium and RTV) through which the heat must flow to reach the heat pipes. NASA LeRC has investigated the possibility of interface phenomena causing the observed anomalies. At TRW we have limited the scope of our investigation - and this report - to the possible role of the heat pipes.

Table 3 presents the results of calculations to determine the thermal resistance between the tube body and the heat pipes under normal and anomalous conditions. The analysis leading to these results is presented in Appendix A. The data permits the following observations:

- The resistance increases prior to the tube body temperature excursion.
- A substantially larger increase in resistance is associated with the excursion itself.
- The resistance returns to the normal range subsequent to the anomaly, indicating no permanent changes.

2.3 ANOMALIES ASSOCIATED WITH ECLIPSE SEASONS

Although the sample size is small, all available evidence suggests that the anomalous behavior is associated with the eclipse seasons. The first three anomalies (days 75, 82, and 101) all fell within the vernal eclipse season (days 55-102), and the fourth anomaly (day 253) fell in the autumnal eclipse season (days 241-288). Furthermore, an eclipse season prerequisite would explain the absence of any anomalies during the first year of operation in 1976. The TEP was not operated during the eclipse seasons of 1976 because of relay problems elsewhere on the spacecraft.

The question then arises as to what distinguishes the eclipse or equinox seasons which could influence the operation of the heat pipes? Two potentially relevant phenomena have been identified. First, the eclipse itself leads to a relatively rapid excursion in system temperatures. Second, the small sun angle during the equinox periods results in lower radiator (and heat pipe condenser) sink temperatures throughout the orbit. This is shown in Figure 7 which plots the maximum and minimum values of sensors HPT5 and HPT6 through the 1976 seasons. (See Figure 1 for sensor locations.)

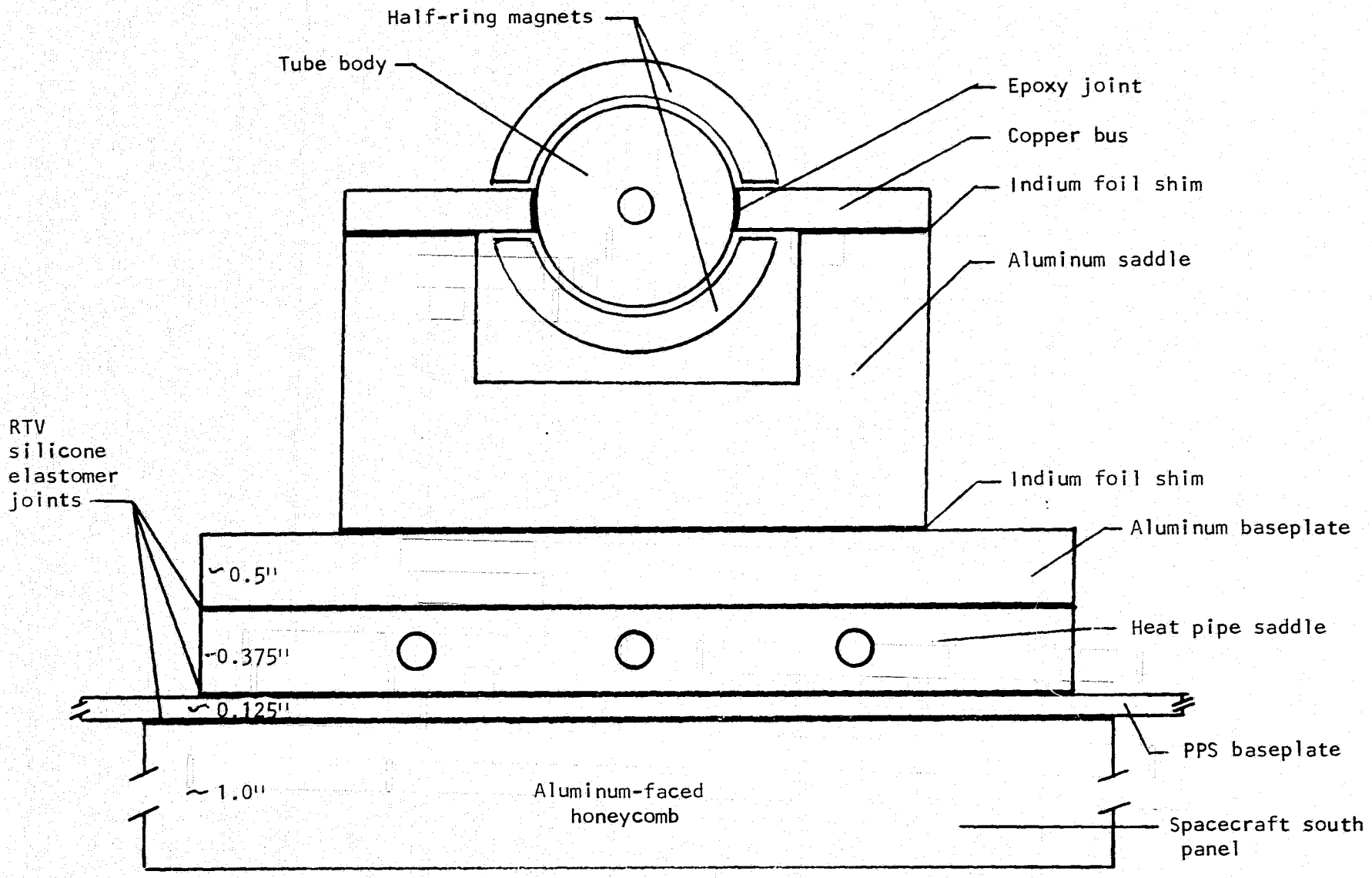

Section A-A
(Schematic-no scale intended)

Figure 6. Mounted CTS OST

Table 3. Thermal Resistance Between Tube Body and Heat Pipes*

Normal Value:** R = 0.14°C/Watt

Anomalies:	Just Prior to Temperature Excursion	Just Prior to Power Reduction
1 (Day 75)	0.17	0.41
2 (Day 101)	0.17	0.38
3 (Day 82)	0.17	0.32
4 (Day 253)	0.15	0.28

*Lumped-Parameter Model: $R = \Delta T/Q_{B.P.}$; ΔT = Tube body minus largest of HPT3, HPT2, and HPT1; $Q_{B.P.}$ = Heat transferred to baseplate.

**Days 74, 81, 89 and 254 at saturation power and similar time of day.

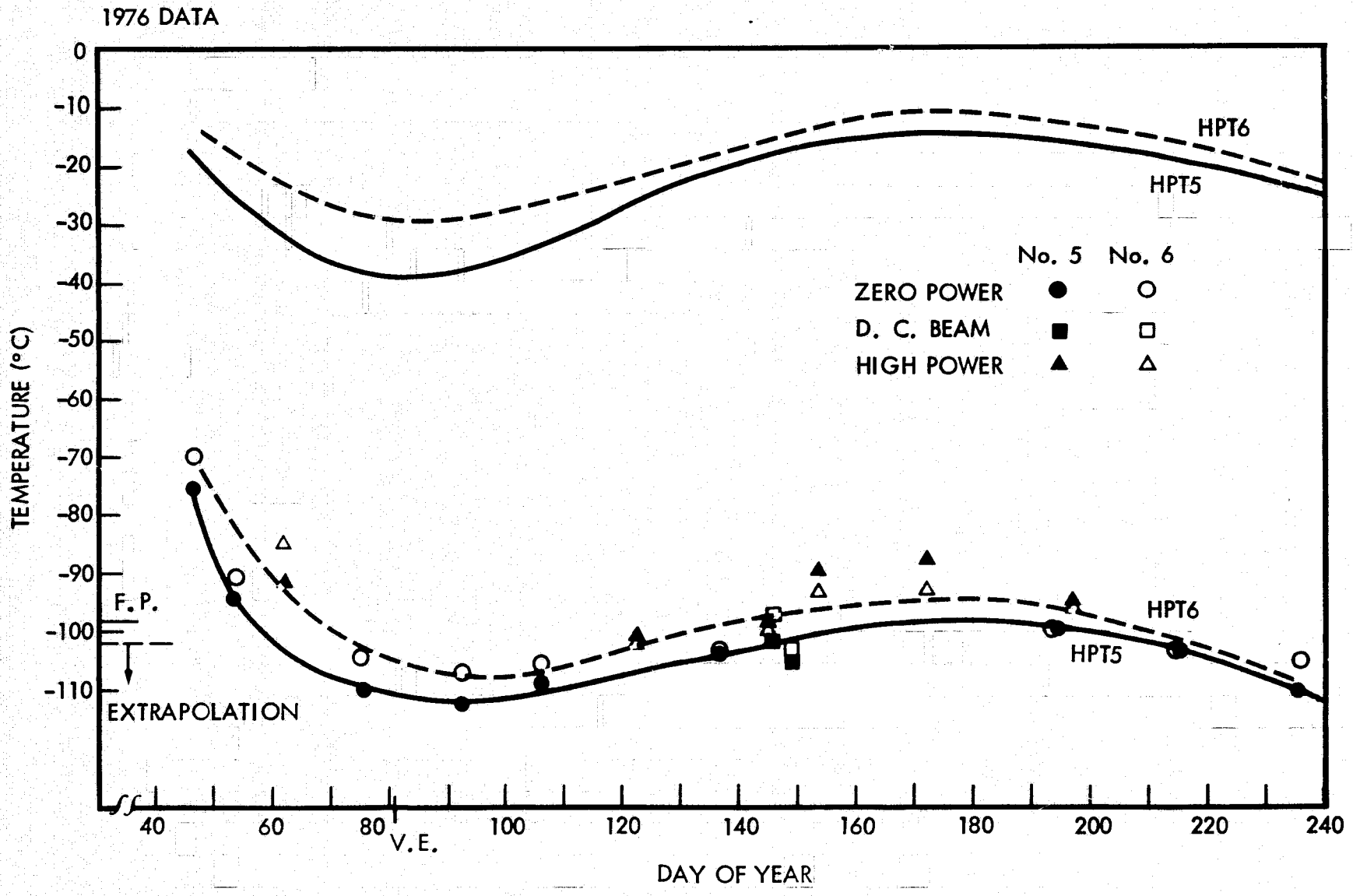

Figure 7. Minimum and Maximum Readings for HPT5 and HPT6 During 1976
(F.P. - Freezing Pointing of Methanol; V.E. - Vernal Equinox)

3. CONSISTENCY OF ANOMALOUS BEHAVIOR WITH HEAT PIPE OPERATING CHARACTERISTICS

3.1 HEAT PIPE CAPACITY

The CTS heat pipes utilize a sophisticated wick system, including two "arteries," to obtain high heat transport capacity as shown in Figure 8. Such heat pipes exhibit multiple capacities, depending on how many of the arteries are "primed"*, as shown in Figure 9. Although the pipes are designed to operate with primed arteries, such operation is metastable. Thus, if something causes one or both arteries to deprime, the heat pipe capacity falls to the single artery or open-artery value, respectively. The open-artery capacity represents a stable operating mode. If the heat load exceeds this value, the heat pipe continues to pump its open-artery capacity while the excess causes an increase in the source temperature.

We can thus associate the observed thermal anomalies with depriming of the heat pipe arteries. Prior to the anomalies the primed heat pipes carry a load in excess of their open artery capacity (see Table 2). A hypothetical depriming of the arteries reduces the capacity below the load and results in an increase in tube body (source) temperature. Decreasing the load to within the open-artery capacity would stabilize operation, and decreasing it further would allow the arteries to reprime and the system to return to normal with no permanent effects.

Qualitatively, the above description is consistent with the CTS observations. Furthermore, a lumped parameter transient analysis of the four anomalies shows that the temperature excursions stabilize to linear rise rates which correspond to a residual heat transfer capacity of about 105-115 watts. This analysis is presented in Appendix B; the results are shown in Table 4.

Values of 105-115 watts substantially exceed the predicted open artery capacity for the system ($\sim$ 60 watts for 3 heat pipes -see Fig. 9).

---

*An artery is primed when it is completely filled with liquid and contains no trapped vapor or gas bubbles within it.

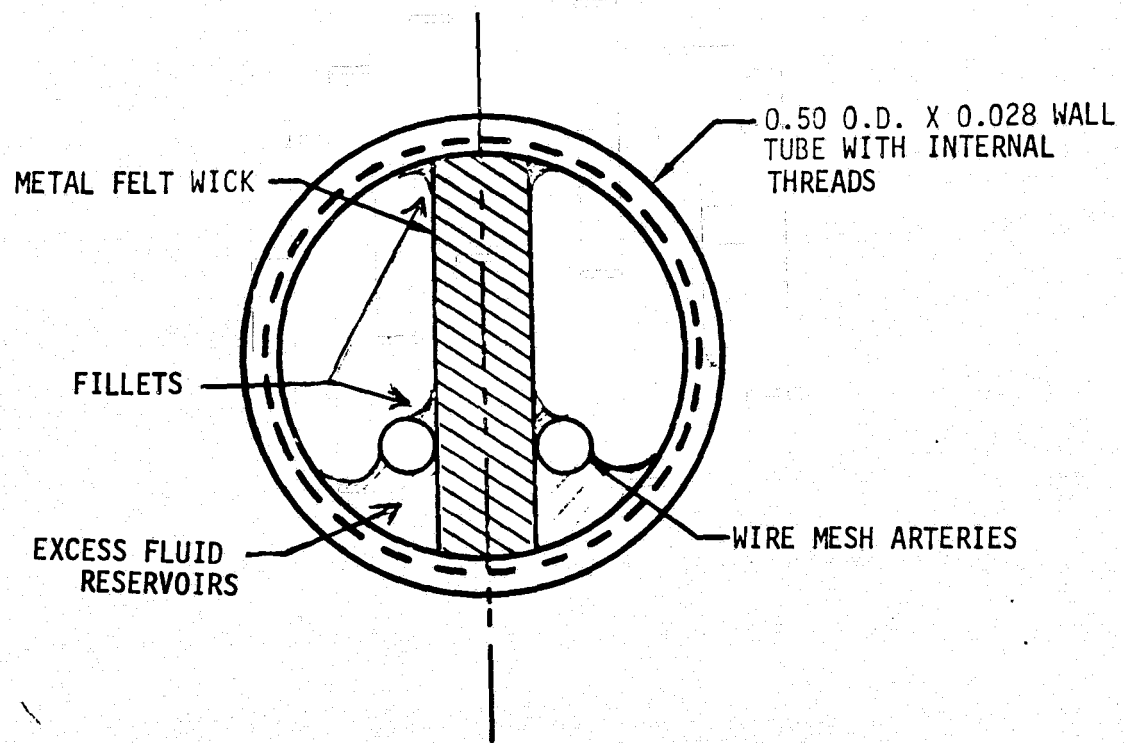

Figure 8. CTS Heat Pipe Wick Configuration

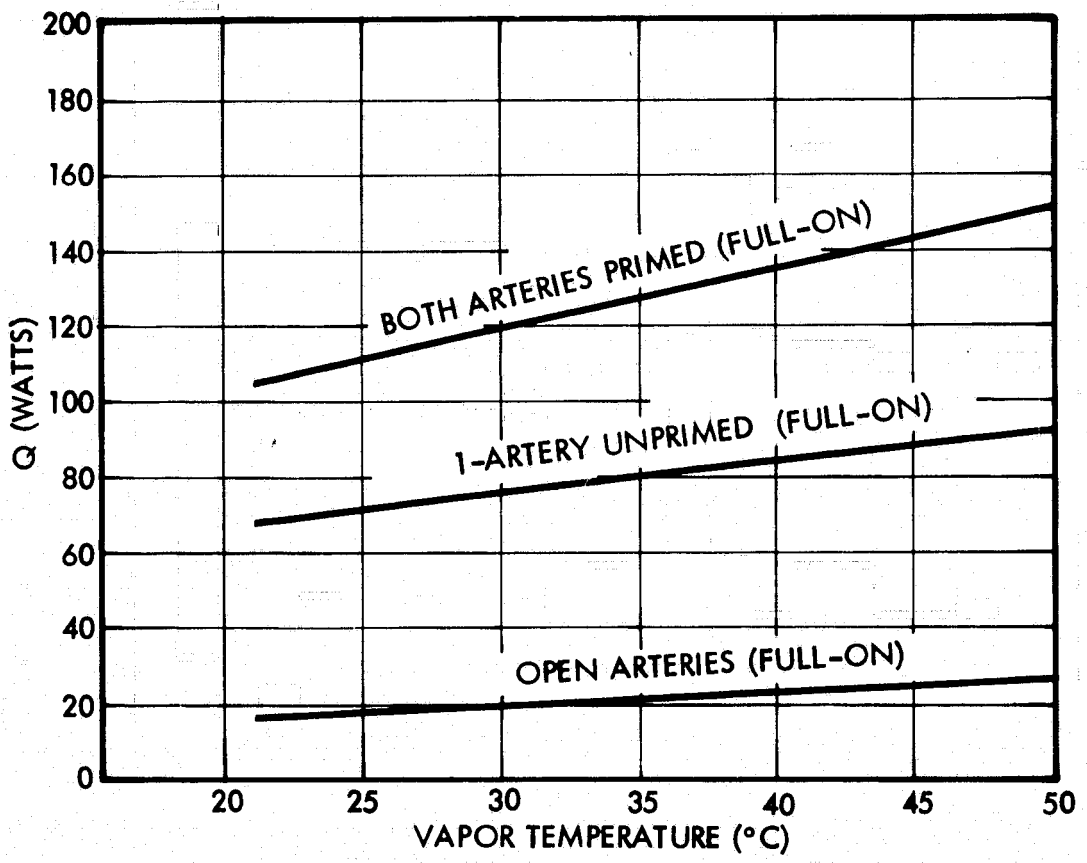

Figure 9. Multiwick Computer Program Predictions for Heat Transfer Capacity of CTS Heat Pipes Under Orbital Conditions (Per Pipe).

Table 4. Results of Transient Analyses of Thermal Anomalies

Anomaly	Dissipated Power (Watts)	$\frac{\Delta T_{Body}}{\Delta t}$ (°C/Min)	Heat Stored (Watts)	Heat Rejected (Watts)
1 (Day 75)	140	0.33	33	107
2 (Day 101)	148	0.41	41	107
3 (Day 82)	121	0.14	14	107
4 (Day 253)	143	0.30	30	113

However, the predictions do not account for several factors including:

- A reduction in effective pumping length due to gas blockage in the condenser and partial dryout of the evaporator will increase capacity over that predicted.
- Marangoni flow in excess fluid reservoirs due to the axial gradient in surface tension in the gas blocked region will decrease capacity with respect to that predicted.

The results shown in Table 4, as well as several direct flight measurements to be discussed later, indicate that the residual heat rejection capacity of the system is in the 100-115 watt range during an anomaly. It is not beyond reason to hypothesize that this corresponds to the open artery capacity of the 3 heat pipes.

3.2 HEAT PIPE THERMAL RESISTANCE

The CTS heat pipes incorporate capillary circumferential grooves to provide a very low resistance to heat flow into and out of the heat pipe (Reference [1]). When wet with liquid, these grooves exhibit a conductance of about 1.5 watts/°C per cm of pipe length. Most of the heat transfer through the tube baseplate occurs over a 7.5 cm length along the pipes. Assuming some spreading by the aluminum heat pipe saddle, we can estimate the conductance from the saddle to the vapor (adiabatic section temperature) at about 40 watts/°C. This yields a resistance of about 0.025°C/watt which, when added to the resistance of 0.14 °C/watt measured in laboratory thermal vacuum tests from the tube body (back-up unit) to the heat pipe saddle, yields a total of ≃ 0.16 °C/watt. This agrees well with the normal operating range measured in orbit with the flight hardware (Table 3).

However, the low heat pipe evaporator resistance is predicated on the circumferential grooves being wet with liquid methanol. If the heat pipe arteries deprime and the load is sufficiently high, the upstream end of the evaporator will dry out, increasing the resistance to heat flow. In fact, a sufficient length of evaporator will dry out such that the heat flow into the pipes is limited to their capability to reject it (open artery capacity).

Thus, we would expect to observe an increase in thermal resistance between the tube body and heat pipes whenever the arteries in a heat pipe

deprime while the pipe is under a load exceeding its open artery capacity. Furthermore, we would expect the resistance to return to normal once the load was removed and the grooves re-wetted.

The behavior observed during the CTS thermal anomalies (Table 3) is consistent with this scenario. The VCHP/Radiator system carries three heat pipes, any two and perhaps one of which can readily carry the full load. If the arteries in one heat pipe deprimed, we would see a small increase in resistance but no thermal runaway. Not until the arteries in the last heat pipe deprimed would we observe a runaway excursion in resistance and tube body temperature until power was reduced.

3.3 HEAT PIPE VAPOR TEMPERATURE

The wall temperature along an adiabatic section of a VCHP is a good measure of the vapor temperature within the active section of the pipe. These are the measurements we make with sensors HPT1, HPT2, and HPT3.

When the heat pipe load is within its capacity and the evaporator grooves are wet, the adiabatic temperature is approximately equal to the evaporator temperature. However, when the load exceeds the capacity and the evaporator grooves dry out, the adiabatic temperature no longer reflects the evaporator temperature but only that of the hottest point at which there is liquid to evaporate. Thus, the pipe will run cooler than the evaporator - at a temperature determined by the sink conditions, the open-artery capacity, and its variable conductance design characteristics.

A review of all flight data has shown a one-to-one correlation between the anomalies and a temperature difference ΔT_{3_1} = HPT3-HPT1 of 5°C-7°C* prior to the excursion in tube body temperature. By contrast, ΔT_{3_1} = 0-3°C at all other times during which all heat pipes were turned on. In fact, it was this observation which led to a scan of all data for $\Delta T_{3\_1} > 5°C$, during which anomaly No. 3 was discovered.

A series of laboratory tests were conducted at NASA LeRC to try to simulate the 5°-7°C spread between HPT3 and HPT1. The tests were performed with the flight back-up VCHP/Radiator System - S/N 004 - and a simulated

---

*This accounts for the recently discovered calibration error in HPT3 which caused all tabulations to indicate HPT3 about 1.7°C too high in the 20°-40°C range.

TWT which provided control of the generated heat distribution. The results of these tests are presented in Table 5.

Two attempts were made to generate the temperature spread by simulating an asymmetric interface failure. In one case all of the heat was generated on the H.P. No. 3 side of the tube and conducted through a uniform interface. In the second case half the tube baseplate (under the H.P. No. 1 side) was removed to force all heat into the No. 3 side of the heat pipe saddle. The steady state ΔT_{3-1} for these cases was only 2.3°C and 2.2°C respectively, indicating that large transverse gradients cannot be generated through asymmetric heating of the heat pipe saddle with all heat pipe arteries primed.

The remaining tests was performed with uniform heating; first with all heat pipes primed and then with No. 1; Nos. 1 and 2, and Nos. 1, 2, and 3 deprimed, respectively. As shown in Table 5, causing heat pipe No. 1 to deprime increases ΔT_{3-1} from 1.1°C to 5.6°C. If both No. 1 and No. 2 are deprimed, ΔT_{3-1} expands to 7.8°C. Note that in both cases the transverse spread in saddle temperature (and hence evaporator temperature) is less than 2.3 °C. Thus, these experiments demonstrated that the large ΔT_{3-1} associated with the flight anomalies is consistent with deprimed arteries in Heat Pipe No. 1 or Nos. 1 and 2 without the need for any transverse gradient in the evaporator saddle or tube baseplate.

3.4 CONDENSER FREEZING UNDER LOAD

The freezing point of methanol - the working fluid in the heat pipes - is -98°C. Figure 7 shows that the reservoir end of the No. 1 heat pipe condenser - as measured by HPT5 - can fall well below the freezing point during the eclipse seasons. Note that the minimum in HPT5 does not occur during the eclipse itself, but some 12-13 hours later (near 180° orbital position) when the radiator is shielded from the sun by the spacecraft.

The temperature to which HPT5 falls depends on the power dissipation and history as well as the season. However, it also appears to depend on whether an anomaly is about to occur. Table 6 shows that for similar time of day during the cold portion of the orbit and similar dissipation rates, HPT5 falls to a lower temperature on days 75 & 101 prior to the anomalies than on days 74, 89, and 254 during which no anomaly occurred.

Table 5. Summary or Results of Simulated-OST/VCHPS Tests

LeRC: 7-26-77 Through 8-10-77

Instrumentation and Reading	TESTS					
	"Normal" All H/P's ON 158 Watt Uniform Heating	Asymmetric Heating All H/P's ON 159 Watts, All ON H/P 3 Side	H/P 1 Failed H/P's 2 and 3 ON 158 Watts, Uniform Heating	H/P's 1 and 2 D Failed H/P 3 ON 158 Watts, Uniform Heating	All H/P's Failed 38 Watts, Uniform Heating	All H/P's ON 158 Watts, All Heat through 1/2 of Tube Base Plate**
HP1, Sdl. °C	51.4	50.8	54.3	59.7	60.0	51.2
HP2, Sdl. °C	51.7	51.4	54.2	59.0	59.3	51.7
HP3, Sdl. °C	52.1	52.8	54.3	57.4	58.6	53.2
HP1, Side °C	49.7	48.9	47.1	46.7	45.6	49.6
HP2, Side °C	49.8	49.7	51.8	50.0	46.9	50.0
HP3, Side °C	51.1	51.8	52.8	55.6	47.9	52.6
HP1, Bot. °C	50.6	49.6	47.9	47.4	45.7	50.2
HP2, Bot. °C	50.2	50.2	52.5	50.7	46.8	50.2
HP3, Bot. °C	49.6	50.4	51.3	54.1	46.5	51.2
BODY °C	84.4	54.4	90.4	107.4	82.2	62.6
HP1T °C	45.4	44.4	44.4	43.3	44.4	47.8
HP2T °C	46.7	46.7	50.0	46.7	45.6	48.3
HP3T °C	46.7	46.7	50.0	51.1	46.7	50.0
HP4T °C	46.7	45.6	46.7	44.4	43.9	48.3

*Thermocouple Electrically Ungrounded

*Turn-on Sequence: 3:2:1

Table 6. Correlation of HPT5 With Incipient Anomaly

Day	Time (E.S.T)	TEPP (Watts)	B.P. Dissipation (Watts)	HPT5 (°C)
74 (No Anomaly)	~12:00	460	152	-80
75 (Anomaly)	~12:00	435	140	-95
89 (No Anomaly)	~12:00	440	142	-83
101 (Anomaly)	~12:30	450	148	-95
254 (No Anomaly)	~12:00	470	157	-82

This behavior can also be explained in terms of artery depriming in H.P. No. 1 prior to the anomaly. The gas loading of the three VCHP's is such that they turn on in sequence at progressively higher evaporator saddle temperatures. Also, at any given normal operating condition below the maximum system design load, H.P. No. 1 will carry the highest load with the vapor-gas front furthest out, followed by No. 2 and then No. 3. Thus, with H.P. No. 1 primed and the system at saturation load, its vapor-gas front is out so far as to keep HPT5 (and perhaps the whole radiator) well above the freezing point. On the other hand, if the arteries in H.P. No. 1 are deprimed (manifested by a spread in ΔT_{3-1} and subsequent anomaly), its vapor-gas front will contract. Although the front positions of Nos. 2 and 3 will extend as they pick up the load, they will not extend as far down the radiator - permitting HPT5 to fall to a lower temperature and perhaps permitting portions of Nos. 2 and 3 (which are colder)* to freeze. The implications of condenser freezing are discussed in Section 4.1.

3.5 FLIGHT EXPERIMENTS MOSTLY CONSISTENT WITH OPEN ARTERY OPERATION

A series of flight experiments were performed to investigate whether the heat pipes were implicated in the thermal anomalies and to explore operational limits and constraints.

The first experiment was performed on day 114 of 1977, prior to TRW's involvement in the investigation. The purpose of this experiment was to determine whether freezing the radiator would deprime the arteries and precipitate the anomaly. The experimental approach was to maintain a zero power condition until the coldest part of the orbit where HPT5 was well below freezing, and then to apply and hold the maximum saturation load. The result was that the VCHP/Radiator system turned on and carried the load for the entire 3-hour test period without any anomaly. Clearly, the freezing protocol followed in this experiment did not deprime the heat pipe arteries. Note that this experiment was not performed during an eclipse season (days 55-102) which now appears to be a prerequisite for suffering an anomaly.

Subsequent flight experiments were performed on days 247, 253, 254, and 283 according to the experiment protocol described in Appendix C.

*One side of the radiator near heat pipe No. 1 is insulated. Thus, the radiator at pipes Nos. 2 and 3 should cool faster.

The specific objectives of these experiments were to determine whether behavior of the system during an anomaly was consistent with heat pipe theory, and to determine the open-artery capacity for fail-safe operation.

An anomaly was recorded on day 253 only, even though nearly identical conditions were established on the other experiment days. However, sufficient data were accumulated on this day to establish the following:

1) The anomaly began before any recorded temperatures approached the methanol freezing point. The lowest temperature was HPT5 =-82°C.

2) After the anomaly began, the tube body temperature rise rate stabilized at 0.30°C/min. before the power was reduced. This corresponds to 113 watts heat rejection through the heat pipes.

3) The tube body temperature stabilized at 70°C with RF_{out} = 130-140 watts watts. This corresponds to 100-106 watts heat rejection throughout the baseplate.

4) Cycling the RF output between 130-200 watts (dissipation between 100-143 watts) caused the tube body temperature to rise and fall. This indicates a stable operating condition with a heat rejection rate somewhere within these limits.

5) By dropping the RF output to zero (D.C. Beam) and allowing the tube body temperature to fall to its normal operating range, the heat pipe evaporators appear to have re-wetted while the condensers were at very low (perhaps frozen) sink conditions. This observation is based on a reduction in thermal resistance from 0.28 °C/watt prior to the first power reduction to 0.16 °C/watt after 70 minutes of operation at RF_{out} = 200 watts following 110 minutes at D.C. beam conditions.

The first observation does not reflect on open artery performance but will be discussed later when considering possible causes of artery depriming. The second through fourth observations are consistent with open-artery operation and suggest a residual heat rejection capacity in the range 100-110 watts.

The fifth observation is troublesome since re-wetting of the heat pipe evaporators does not seem probable if the free methanol in the heat pipe is frozen.

3.6 HYPOTHETICAL PERFORMANCE MODEL

The operational characteristics of the CTS heat pipes can be qualitatively represented as shown in Figure 10. Operation with unprimed arteries is stable but limited to low heat transfer capacity. If the load exceeds point **A**, the evaporator begins to dry out at the upstream end and the thermal resistance of the system increases rapidly. If the arteries are primed, the heat transfer capacity is very high (Figure 9) and the system exhibits a low thermal resistance under all operating conditions. However, beyond point A primed artery operation is metastable. Should the arteries deprime at a load exceeding "A" the capacity falls to the unprimed artery curve and the tube body temperature increases along with the resistance due to the excess load.

In view of this behavior, the observations we have made regarding the characteristics of the thermal anomalies and the results of laboratory and flight experiments are, for the most part, consistent with the following hypothetical model:

1) The thermal anomaly corresponds to the depriming of the heat pipe arteries, causing the evaporators to dry, the resistance to increase and the tube body temperature to rise.

2) Heat pipe No. 1 (and perhaps heat pipe No. 2) deprimes before heat pipe No. 3, yielding the characteristic increase in HPT3-HPT1 from <3°C to >5°C preceding the anomaly. This increase is due to the increase in thermal resistance from the common heat pipe saddle to the H.P. No. 1 vapor as a consequence of evaporator dryout. This also shows up as a small increase in the overall resistance from the tube body to the heat pipes.

3) The residual heat transfer capacity of the system during the anomaly is the open artery capacity of the heat pipes. It is a weak function of the tube body temperature, depending on the extent of evaporator dryout (it lies between points A and B on

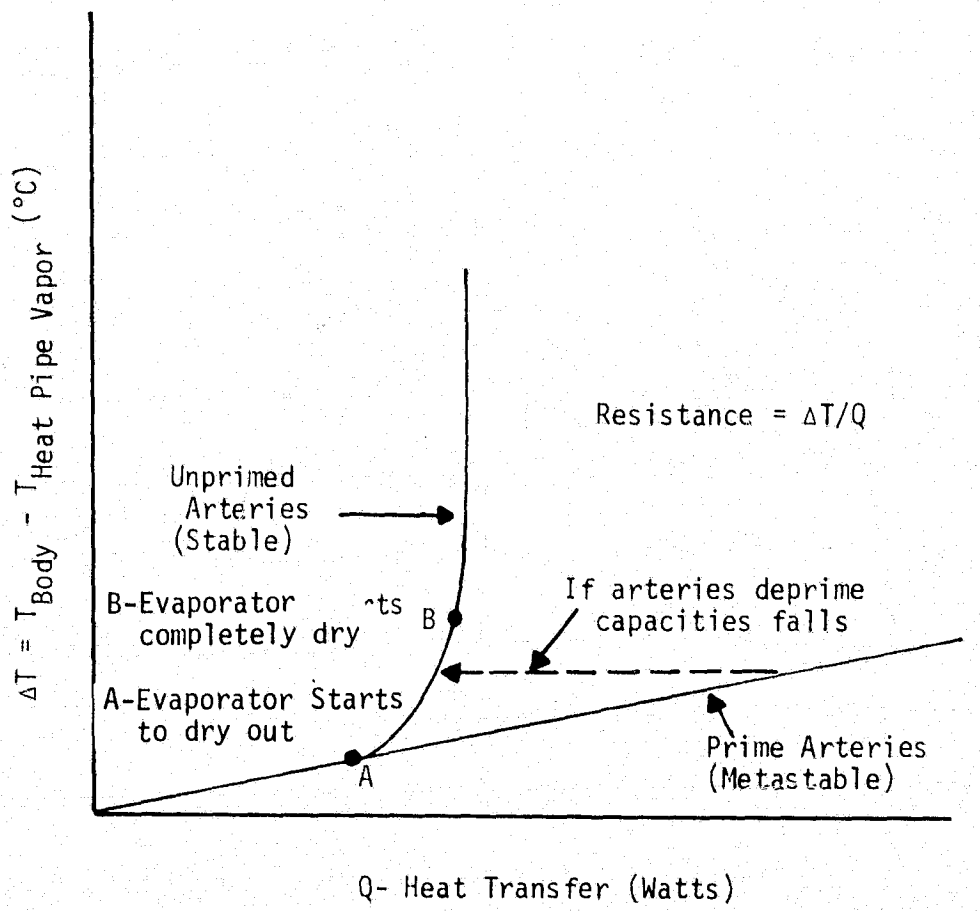

Figure 10. Qualitative Representation of Heat Pipe Performance

on Figure 10). It may also vary with the quantity of liquid methanol available in the pipe when a portion of the condenser is frozen and with Marangoni flow effects (Section 4.2). Typical values appear to be 100-113 watts.

4) When the load on the heat pipes is removed and there is liquid methanol available, the arteries automatically reprime and the system again exhibits "normal" behavior.

The one observation which may be inconsistent with this artery depriming-repriming mechanism is that, by reducing the load, the thermal resistance of the system substantially recovers on day 253 - and also on day 101 - before the radiator begins to warm from the coldest orbit position. If the radiator is frozen under these conditions (HPT5 is in the range -95° to -102°C), it would seem likely that the excess methanol would be tied up in the solid state and not be available to re-wet the evaporator and lower the resistance.

In spite of this uncertainty the preponderance of evidence supports the depriming - repriming hypothesis. The problem then remains to understand what causes the arteries to deprime in the first place.

4. ARTERY DEPRIMING MECHANISMS

The most perplexing aspect of explaining the anomalies in terms of heat pipe behavior is to identify a cause for the arteries to deprime which is consistent with all of the data. It is not necessary to find a single mechanism by which all arteries deprime to cause an anomaly. Multiple mechanisms which are dependent on each other and lead to sequential depriming would be equally plausible. However, to invoke multiple mechanisms which are independent of each other to explain depriming of different pipes during a given anomaly or depriming during different anomalies seems very improbable.

Whatever mechanisms we identify for artery depriming must be consistent with three key observations:

1) The anomalies occur only during the eclipse seasons.

2) The anomalies are sporadic. Similar conditions on successive days can yield an anomaly on one day and not the next.

3) The anomalies are triggered by the depriming of the arteries in H.P. No. 1. (See Section 3.3.)

The most obvious cause of artery depriming in a heat pipe would be for the heat load to exceed the heat transfer capacity of the pipe. This is clearly not the cause in our case since: (1) the heat loads are well below the system capacity when the arteries are primed, and (2) on many days surrounding the anomalies, higher heat loads were accommodated without difficulty.

A vibration or acceleration load in excess of that which can be sustained by the maximum capillary head would also cause depriming. But this too must be discarded since no such loads are present - certainly not any which are unique to the eclipse seasons. Attitude control thrusters impart very low acceleration loads and do so all year.

Similar disclaimers can be made for mechanical failure, chemical degradation of the methanol, corrosion, etc. All would yield permanent rather than sporadic effects and would not be tied to the eclipse seasons.

Our investigation identified only three mechanisms which would be associated with the eclipse seasons: (1) condenser freezing, (2) Marangoni flow, and (3) gas evolution due to rapid chilling. These are discussed in the following sections.

4.1 CONDENSER FREEZING

It has been previously demonstrated that, under certain conditions, freezing the condenser of the CTS heat pipes can lead to artery depriming (Reference [1]). Two mechanisms had been identified which would transport mass from the evaporator to the condenser where it would freeze and not be available for recirculation: (1) vapor diffusion (diffusion-freezout), and (2) liquid pumping in the fillets and natural excess fluid reservoirs due to the decrease in liquid specific volume (increase in density) as it cooled. A third mechanism - Marangoni flow - has recently been identified and will be discussed in the next section.

Simply freezing the heat pipe condensers with the system under no load does not necessarily deprime the arteries. This was demonstrated by the flight experiment on day 114 (Section 3.5). A prerequisite appears to be that the fillets and excess fluid reservoirs in the thawed portion of the pipe be depleted of liquid and unable to resupply the wick and arteries as additional working fluid is bound up as ice. This requires that freezing take place while the system is under load. However, too high a load will prevent the radiator from freezing.

This model - the need for a heat load but not too high a load - could account for the sporadic occurrence of anomalies. Furthermore, the particularly low sink temperatures associated with the eclipse seasons (Figure 7) may be necessary to open a window between the minimum required and maximum tolerable loads, explaining the seasonal limitation. However, several other factors imply that, although condenser freezing can and may lead to artery depriming, it is not the primary cause of the anomalies. These are as follows:

- Anomaly No. 4 occurred before heat pipe No. 1 approached freezing conditions.
- With all pipes primed heat pipe No. 3 should freeze and deprime first since it carries least load and its fin radiates from both

sides. However, heat pipe No. 1 is the first to deprime.

- Under saturation load, such as existed during anomalies Nos. 1 and 2, it appears that the condenser of heat pipe No. 1 can reach freezing conditions only after the arteries have already deprimed (Section 3.4).
- Following an anomaly, the system can recover its normal thermal resistance before the radiator begins to warm up. If sufficient excess fluid was frozen to cause artery depriming there would be none available to re-wet the evaporator.

4.2 MARANGONI FLOW

Marangoni flow refers to the motion of fluid which results due to a gradient in surface tension References [2,3,4,5.] It has been suggested by NASA LeRC personnel that the temperature gradient along a VCHP in the gas blocked region would yield a surface tension gradient which, in turn, would cause a surface flow toward the condenser end along all continuous vapor-liquid interfaces. In particular, a surface flow would be induced along the fillets and excess fluid reservoirs but not in the wick or arteries which do not have free vapor-liquid interfaces along the length of the pipe.(See Figure 8.)

Consideration of Marangoni flow effects suggests two mechanisms by which the behavior of the CTS heat pipes could be influenced, as follows:

1) If the end of the condenser were frozen, the flow along the free surfaces would enhance the accumulation of ice at the condenser and the depletion of the fillets and excess fluid reservoirs at the evaporator. This would increase the probability of depriming the arteries by freezing. However, the contribution of Marangoni flow does not remove the objections to freezing as the primary depriming mechanism which were enumerated in Section 4.1.

2) If the heat pipe is not frozen, Marangoni flow still results in surface flow towards the end of the condenser. By continuity, however, there must now be a return flow beneath the surface and an associated liquid pressure drop. The net effect of the surface tension gradient will be to reduce the contribution which the fillets and excess fluid reservoirs make to the capacity of the

heat pipe. This effect cannot be large enough to deprime the arteries. If it were, we would experience anomalies on consecutive days under similar conditions and not sporadically as we do. However, once an anomaly has occurred, the Marangoni effect probably has a measurable influence on the open artery capacity of the heat pipes, causing some of the variation we see (Section 3.6).

4.3 GAS EVOLUTION WITHIN ARTERIES

The CTS heat pipes contain a 90 percent nitrogen -10 percent helium gas inventory to provide their variable conductance control function. The solubility of this control gas in the methanol working fluid is a function of both pressure and temperature, decreasing as they fall. This temperature and pressure dependence of solubility gives rise to a potential artery depriming mechanism which is consistent with sporadic occurrences during the eclipse season. The scenario is as follows:

1) TEP operations cease several hours before an eclipse. This causes the evaporator temperature and heat pipe pressure to fall sufficiently so that the gas blocked region expands to fill the entire pipe length.

2) Over the next several hours the liquid in the arteries becomes saturated with the gas surrounding them at the existing temperature and pressure.

3) When the spacecraft enters the eclipse, the heat pipes experience a rapid chilldown. This causes a decrease in their internal pressure.

4) The decrease in both liquid temperature and gas pressure render the liquid supersaturated in dissolved gas. We hypothesize that the supersaturation is sufficient to nucleate gas bubbles within the arteries.

5) Gas is evolved at numerous nucleation sites, leading to many small bubbles. We now hypothesize that many of these bubbles coagulate to form fewer but larger bubbles with a lower overall surface-to-volume ratio.

6) When the spacecraft comes out of eclipse and the heat pipes warm up again, the rate at which the gas redissolves into the liquid due to the now-higher solubility is slow because of the small surface-to-volume ratio of the large bubbles. Furthermore, since gas is also available to the liquid in the arteries from the vapor space surrounding them, the liquid can become re-saturated before the bubbles are completely redissolved.

7) When TEP operations are initiated following the eclipse the heat pipes will "turn on" with the formation of a vapor-gas front and the buildup of stress in the liquid (P_v-P_l). The bubbles within the arteries in the active portions of the pipes will then tend to: (1) dissolve by diffusion of gas to the now-gas-free vapor space, and (2) vent through the priming foils if they are converted upstream by the flowing liquid. However, if the load on the heat pipes increases too quickly, such that the local liquid stress exceeds $2\sigma/r_{bubble}$ before the bubbles are dissolved or vented, the arteries will deprime.*

The hypothesized scenario suggests that gas bubbles may be generated within the heat pipe arteries every day during the eclipse period, but gas bubbles are only detrimental if they are in the active zone of the pipe where they can grow or be converted upstream. Hence, we are only concerned with those days during which there was a sufficient period of time prior to the eclipse when the heat pipes were fully off for the gas to saturate the arteries along their entire length. If, however, conditions are such that on most days bubbles are either not formed in the active zone or are eliminated by diffusion or venting before a high enough load is established to cause depriming, this would explain the sporadic occurrence of the anomalies.

---

*A gas bubble within an artery will grow in size if the pressure difference between the gas-vapor mixture within it and the local liquid surrounding it exceeds $2\sigma/r_{bubble}$ where σ is the surface tension and r_{bubble} is the radius of the bubble (or the bubble end cap if the bubble fills the artery diameter and takes on a sausage-shape). If the bubble grows into (or is convected into) the priming foil region - and if the local stress is high enough, vapor will enter the artery causing it to deprime rather than be vented from it. Detailed discussions of bubble behavior in arteries and priming foils will be found in References [6, 7 and 8]. Reference [8] is reproduced in this report as Appendix D because of limited availability in the literature.

Of all the possible artery depriming mechanisms identified, the gas evolution mechanism seems most plausible. It ties the anomalies to the eclipse seasons when the system experiences rapid chilldowns. It also provides an explanation for sporadic occurrences within the eclipse season since: (1) it depends on the operating conditions before and after the eclipse, and (2) bubble nucleation and agglomeration are statistical phenomena.

4.3.1 Nucleation Experiment

Analytical treatment of the gas evolution scenario would be extremely laborious and not particularly fruitful. The theory of bubble nucleation centers around the pre-existence of nucleating sites whose size can only be estimated within one or two orders of magnitude - yielding inconclusive predictions. Consequently, we elected to perform a simple experiment to determine whether gas bubbles would be nucleated in the arteries under CTS conditions.

The experimental sample consisted of a small section (≈3 inches) of CTS-type wick (Figure 8) inserted into a glass tube sealed at one end and valved at the other. The sample was evacuated and back-filled with 0.4 psia of helium, 3.6 psia of nitrogen and an appropriate quantity of methanol, simulating the CTS design parameters. This "glass heat-pipe" was then immersed in a glass-walled methanol bath with back lighting so that one could observe the liquid in the arteries through a stereo microscope. A series of experiments were then performed to see whether bubbles could be generated within primed arteries by rapid temperature reductions. To aid in detection the sample was tilted longitudinally to put the primed arteries under a hydrostatic stress exceeding their open artery capacity. Thus, if a large enough bubble were to form, the artery would deprime and be unable to reprime - assuring detection. Furthermore, the imposed hydrostatic stress is equivalent to increased supersaturation which enhances the probability of bubble formation.

A typical experimental sequence was as follows:

1) The arteries were primed and the sample tilted .
2) The bath was set at an initial temperature T_o and allowed to rest for a sufficient time to saturate the liquid with gas.

Initial temperatures of -20°C and +23°C were used. Saturation periods were approximately 18 hours (overnight).

3) The bath was rapidly chilled while the arteries were observed through the microscope. In one case the bath was chilled from +23°C to -49°C in 42 minutes. In another case from -20°C to -53°C in 37 minutes.

The experiments yielded negative results. In no case were any bubbles seen within the primed arteries, and in no case did the tilted arteries deprime. Since the cooling rates employed were approximately twice those seen in orbit, and since the artery tilt enhanced the probability of nucleation, we must conclude that this mechanism does not cause artery depriming under the conditions experienced by the CTS.

4.4 SUMMARY

We have not been able to identify any single or sequential series of mechanisms for artery depriming which is consistent with all of the flight data. Of the three mechanisms identified which would be associated with the eclipse seasons, condenser freezing, Marangoni flow and gas evolution within the arteries, only condenser freezing under load has been experimentally shown to result in artery depriming in laboratory tests. However, as discussed in Section 4.1, condenser freezing cannot be the cause of all the anomalous behavior. Marangoni flow effects, while clearly present, do not directly influence flow in the closed arteries and thus can cause only a minor decrease in primed artery capacity - certainly not sufficient to cause depriming. Depriming due to gas evolution within the arteries under rapid chilling of gas-saturated liquid during the eclipse is qualitatively consistent with all observed behavior. However, laboratory attempts to produce gas bubbles within arteries under conditions even more stringent than observed in flight were unsuccessful.

If artery depriming in the heat pipes is the cause of the anomalous thermal behavior, which is consistent with the bulk of the observed data (Section 3), then the factors which cause the arteries to deprime have yet to be identified.

5. REFERENCES

1. P.R. Mock and B.D. Marcus, "TEP Variable Conductance Heat Pipe System," Final Report 4761-TEP-320, Contract NAS3-15839. Also, P.R. Mock, B.D. Marcus and E.A. Edelman, "Communications Technology Satellite: A Variable Conductance Heat Pipe Application," J. of Spacecraft and Rockets, Vol. 12, No. 12, December 1975.

2. V.G. Levich and V.S. Krylov, "Surface-Tension-Driven Phenomena," Annual Review of Fluid Mechanics, Vol. 1, Annual Reviews, Inc., 1969.

3. L.E. Schriven and C.V. Sternling, "The Marangoni Effect," Nature, Vol. 187, July 16, 1960.

4. C.S. Yih, "Fluid Motion Induced by Surface Tension Variation," The Physics of Fluids, Vol. II, No. 3, 1968.

5. S. Ostrach and A. Pradhen, "Surface-Tension Induced Convection at Reduced Gravity," AIAA, January 1977. Also, Case Western Reserve University FTAS/TR-76-123, 1976.

6. B.D. Marcus, D.K. Edwards and W.T. Anderson, "Variable Conductance Heat Pipe Technology - Research Report No. 4," NASA CR-114686, December 1973.

7. J.E. Eninger, "Menisci Coalescence as a Mechanism for Venting Noncondensable Gas From Heat-Pipe Arteries," AIAA Paper 74-748, 1974.

8. J.E. Eninger, "Priming Studies With a Glass Heat Pipe," TRW Report No. 26263-6009-RU-00, January 8, 1975.

PRECEDING PAGE BLANK NOT FILMED

APPENDIX A

THERMAL RESISTANCE CALCULATIONS

Under steady state operating conditions the heat transfer from the tube body to the heat pipes can be characterized by a simple lumped-parameter model, as follows:

$$Q_{B.P.} = (T_{BODY} - T_{HEAT\ PIPE})/R \qquad (1)$$

where

$Q_{B.P.}$ = Heat transferred to baseplate and heat pipes

T_{BODY} = Temperature of tube body

$T_{HEAT\ PIPE}$ = Highest of HPT1, HPT2, and HPT3

R = Thermal resistance between tube body and heat pipes

In Equation (1) we assume that (a) all heat transferred to the heat pipes comes from the tube body dissipation, and (b) all heat transferred to the baseplate enters the heat pipes. We neglect heat conduction through the south panel and radiation from its surface. Although this quantity is small, it renders Equation (1) valid only for relatively large heat transfer rates. The highest value of HPT1, HPT2 and HPT3 is chosen for the heat pipe temperature to eliminate any effects of gas blockage on the measured adiabatic section temperatures of the three pipes.

Equation (1) was used to calculate the effective thermal resistance -R for (1) normal operating conditions, (2) just prior to the anomalous temperature excursions, and (3) just prior to reducing power during the anomalies. Heat dissipation rates were obtained from measurements of the TEPP power and Figure 5. Under steady-state conditions $Q_{B.P.}$ was set equal to the heat dissipation rate. However, under transient conditions during the anomalies, $Q_{B.P.}$ was obtained from the transient analysis presented in Appendix B. The results of the calculations are presented in Table A-1.

Table A-1. Thermal Resistance Calculations

	$Q_{B.P.}$ (watts)	T_{BODY} (°C)	$T_{H.P.}$* (°C)	R (°C/watt)
Normal Operation:				
Day 74 (13:10)	152	54.0	32.8	0.14
Day 81 (13:15)	154	52.0	31.0	0.14
Day 89 (12:30)	146	50.8	30.8	0.14
Day 254 (11:05)	157	56.0	33.8	0.14
Just Prior to Temperature Excursion:				
Day 75	140	56.1	32.7	0.17
Day 82	121	51.3	30.8	0.17
Day 101	148	57.7	32.7	0.17
Day 253	143	51.5	31.0	0.15
Just Prior to Power Reduction:				
Day 75	107	74.7	30.8	0.14
Day 82	107	62.9	29.0	0.32
Day 101	107	71.6	30.8	0.38
Day 253	113	64.0	32.3	0.28

*1.7°C was subtracted from recorded values of HPT3 to account for a calibration error in data reduction.

APPENDIX B

TRANSIENT THERMAL ANALYSIS OF ANOMALIES

Under transient anomalous conditions, when the tube body temperature is rising, a lumped-parameter energy balance on the tuby body gives:

$$Q_{DISSIPATED} = Q_{B.P.} + Q_{STORED} \quad (1)$$

The heat stored in the tube body causes the temperature to rise according to:

$$\frac{dT}{dt} = Q_{STORED}/MC_p \quad (2)$$

where MC_p is the thermal capacity (mass x specific heat) of the tuby body. Laboratory tests of the tube at NASA LeRC indicate that the lumped parameter thermal capacity is MC_p = 101°C/min. Thus, we can rewrite the heat balance as:

$$Q_{B.P.} = Q_{DISS} - 101 \frac{dT}{dt} \quad (3)$$

Applying Equation (3) to the temperature rise rates at the start of the excursion and the time of power reduction for the four anomalies yields the data presented in Table B-1.

Table B-1. Heat Distribution During Anomalies

Anomaly	TEP Power (watts)	Q_{DISS} (watts)	Start of Temperature Rise		Time of Power Reduction	
			dT/dt (°C/min)	$Q_{B.P.}$ (watts)	dT/dt (°C/min)	$Q_{B.P.}$ (watts)
1 (Day 75)	435	140	1.37	2	0.33	107
2 (Day 101)	450	148	1.52	-6	0.41	107
3 (Day 82)	395	121	0.46	75	0.14	107
4 (Day 253)	440	143	0.48	95	0.30	113

The results in Table B-1 indicate that in all four anomalies the heat transferred to the base plate stabilizes at about 110 watts after a period of time. This appears to correspond to the open (unprimed) artery heat transfer capacity of the system.

The data also shows distinctly different behavior during the initial portion of the temperature excursions for the first two anomalies as compared with the latter two. On days 75 and 101, the initial temperature rise rate corresponds to essentially all of the dissipated heat being stored in the tube body with approximately zero transferred out the heat pipes. However, on days 82 and 253, the initial rise rate is much slower and the heat transferred through the pipes -- although below their open artery capacity -- is substantial.

This behavior is not inconsistent with an artery-depriming model as the cause of the anomalies. When an artery deprimes, the liquid within it flows back toward the condenser end. Depending on the stress distribution in the pipe prior to artery depriming, the liquid in the arteries will recede back to various positions along the pipe. This is shown in Figure B-1. In all cases the liquid initially recedes at least to the point where the stress equals the maximum value (capillary head) for unprimed arteries, and probably further due to inertial effects. However, if the pipe is initially under high load (and high stress) prior to artery depriming, the point of S_{max} for unprimed arteries will be further downstream (curve A versus curve B). Thus, the extent to which the arteries -- and hence the wick, grooves, etc. -- dry out upon depriming depends on the initial stress conditions. This will give rise to a variable capacity for heat transfer immediately after depriming.

Once deprimed, the VCHP/radiator system will adjust to the reduced throughput and the arteries will refill with liquid until an equilibrium condition is reached based on their open-artery pumping capacity (curve C). This is consistent with the essentially equal $Q_{B.P.}$ values for all anomalies at the time of power reduction.

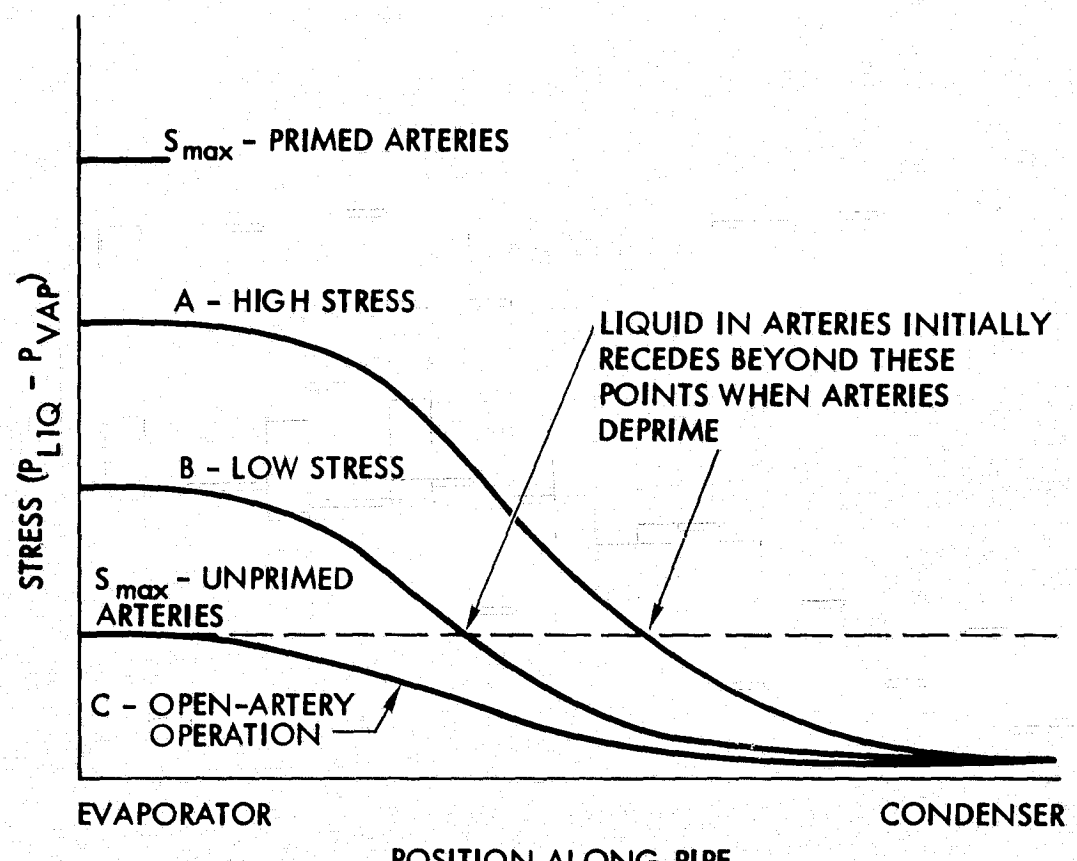

Figure B-1. Model for Stress Dependence of Liquid Recession Upon Depriming of Arteries

APPENDIX C

EXPERIMENT PROTOCOL FOR FLIGHT TESTING OF CTS HEAT PIPES

AUGUST 29, 1977

CONTRACT NAS 3-21012

PREPARED FOR

NASA LEWIS RESEARCH CENTER
21000 BROOKPARK ROAD
CLEVELAND, OHIO 44135

EXPERIMENT PROTOCOL FOR FLIGHT TESTING OF CTS HEAT PIPES

TRW has been participating in an investigation of the possibility that the heat pipe system was involved in the thermal anomalies observed on days 75, 82 and 101 of this year. Analysis of both flight and ground test data suggest that if the heat pipes are implicated:

1) The thermal anomaly corresponds to depriming of the heat pipe arteries, yielding a sudden rise in tube body temperature.

2) Heat pipe No. 1 (and perhaps heat pipe No.2) deprimes before heat pipe No. 3, yielding a characteristic increase in THP3-THP1 from <6°C to >7°C preceding the anomaly.

3) Depriming of the heat pipe No. 3 arteries (and perhaps those in heat pipes Nos. 1 and 2) is due to freezing of the methanol in the condenser while the system is under load. This condition only appears possible during the equinox periods when the radiator sees minimum sink conditions.

As part of the continuing investigation into the cause of the observed anomalies, TRW proposes that several flight experiments be performed with the CTS spacecraft to verify whether the hypothesized heat pipe failure scenario is correct and to explore operational limits and constraints.

The period of the year around the autumnal equinox corresponding to days 75 through 101 around the vernal equinox includes days 247 through 273 (Sept. 4 - Sept. 30). This appears to be the best window to try to reproduce the anomalies observed earlier in the year.

A flow diagram of the proposed experiment protocol is attached. The experiment can be performed in either of two modes - scheduled or unscheduled. Since the previous flight data have shown a one-to-one correspondence between THP3 - THP1 increasing to greater than 7°C and a subsequent anomaly, we recommend that this temperature difference be monitored and used as a flag to transfer spacecraft control to CRC or LeRC and begin the experiment. This would only be done if the flag occurred before 17:00 hours so that the appropriate heat load could be established while the condensers were still freezing. Otherwise, the RF output power should be limited to $\leq$ 130 watts for the remainder of daily operations. This is currently believed to correspond to the open (deprimed) artery heat rejection capacity of the heat pipe system which precludes the thermal anomaly.

It is possible, however, that we could pass through the entire Sept. 4 - Sept. 30 period under normal spacecraft operation without ever observing THP3 - THP1 > 7°C. Thus, on the chance that the depriming of heat pipes Nos. 1 and 2 (leading to the > 7°C Δ T)

and the subsequent depriming of heat pipe No. 3 (leading to the anomaly) are coupled events, we propose that one or more attempts be made to promote the anomaly and run the experiment on a scheduled basis. In these cases the tube D.C. beam should be turned on at 8:00 E.S.T. and the RF output power set to 200 watts at 9:00 E.S.T., after which the experiment sequence is the same as for an unscheduled experiment. The specified power profile will assure that the heat pipes freeze while under high load.

The 200 watt RF output power should be held steady until an anomaly occurs or the experiment is terminated at 19:00. If an anomaly occurs (T_B > 70°C) the RF output power should be reduced to 130 watts. This is believed to correspond to the open (deprimed) artery capacity of the heat pipe system so that the tube body temperature should begin to fall back to a temperature below 65°C. If it does not, we reduce the RF output power in 20 watt increments until it does. The purpose of this sequence is to determine the actual open artery capacity under which the system can operate in a fail-safe mode without possibility of a heat-pipe-artery-failure-induced thermal anomaly.

Upon recovery, the RF output power should be raised back to 200 watts and the tube body temperature monitored. With deprimed heat pipe arteries, the body temperature should again rise above 70°C. If it does not, after operating for at least two hours and until $\geq$ 19:00, the heat pipe arteries will have to have reprimed while under load and with the condenser frozen (unlikely), or the anomaly is caused by something other than the heat pipes.

If the body temperature does rise above 70°C, reduce RFOUT to zero (D.C. beam) and wait until HPT2 < HPT1 -5°C. This condition corresponds to shutting off heat pipes Nos. 3,2 and most of 1, reducing the load low enough to assure artery repriming if sufficient methanol is available in the liquid state. If the condenser is thawed at this point in time (HPT5 > -80°C), the arteries should reprime, and increasing RFOUT to 200 watts should not result in an anomaly. If the radiator is still frozen the arteries may not reprime under low load, and the anomaly will again accompany an increase in RFOUT to 200 watts. In this case the RFOUT = 0/HPT2<HPT1 -5°C/RFOUT = 200 watts sequence should be repeated until the system either operates without an anomaly or fails to do so even after the radiator has thawed (HPT5>-80°C). The purpose of this last sequence of steps is to explore artery repriming under low load and both frozen and non-frozen condenser conditions. We expect that condenser thawing is necessary for repriming. However, the flight data of day 101 suggest this may not be the case.

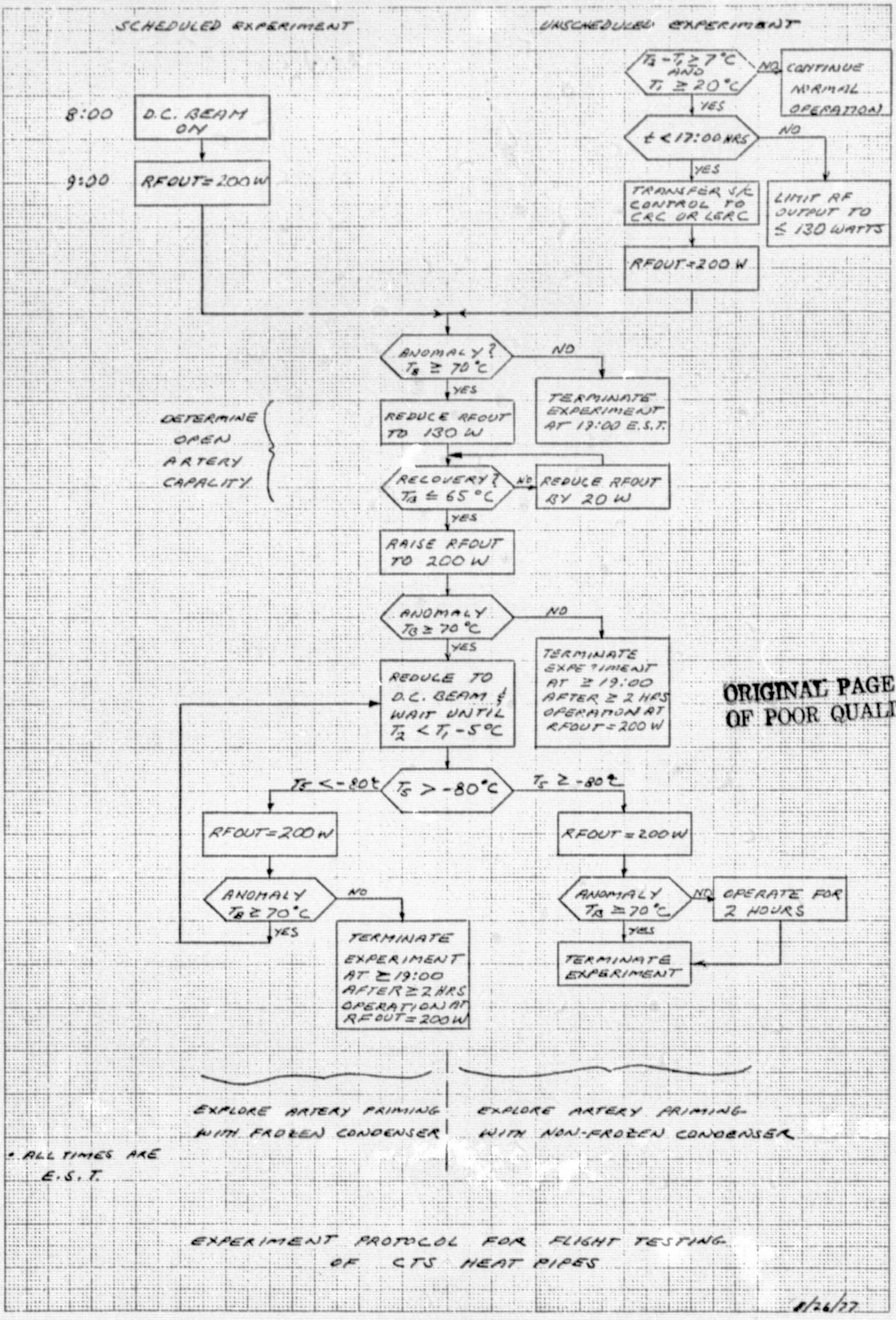

EXPERIMENT PROTOCOL FOR FLIGHT TESTING OF CTS HEAT PIPES

8/26/77

ORIGINAL PAGE IS OF POOR QUALITY

APPENDIX D

Priming Studies with a Glass Heat Pipe

TRW Sales No. 26263
Contract NAS 2-8310
Flight Data Analysis and Further
Development of Variable-Conductance
Heat Pipes

by

James E. Eninger

January 8, 1975

Materials Technology Department

TRW
DEFENSE AND SPACE SYSTEMS GROUP
ONE SPACE PARK • REDONDO BEACH, CALIFORNIA 90278

1. INTRODUCTION

The purpose of the glass-heat-pipe research was to answer some crucial questions regarding a method of priming heat-pipe arteries in the presence of noncondensable gas. This method was successfully tested for the first time in zero gravity by the two research heat pipes provided by Ames Research Center for the October 4, 1974 sounding-rocket launch of the International Heat Pipe Experiment [1]. Priming is accomplished by venting the noncondensable gas, which would otherwise form an arterial bubble, through capillary-sized holes in a foil-walled section of the artery at the evaporator end [2]. Besides heat pipes for the sounding-rocket experiment, the priming method is used on heat pipes for the Communications Technology Satellite [3] and a TRW spacecraft.

Several questions on the priming method required visual observation for answers. The most important unanswered question was why the computer-predicted fluid change is insufficient for the arteries to prime. The glass heat pipe was used to uncover the source of the problem and to test a solution. Other questions were:

- Is a heat load sufficiently low for priming still high enough to convect an arterial bubble along the artery and into the priming foil where it would vent?
- Can excess liquid arrive at the priming foil, submerge it, and thus prevent gas venting before the artery has primed?
- If a bubble is prevented from venting because the foil is submerged, will application of a heat load result in recession of the excess liquid and venting of the bubble?

2. DESIGN AND FABRICATION OF APPARATUS

As shown in Figure D-1, the main component of the apparatus is a 1.9-cm O.D. (0.752-inch-I.D.) 1.3-cm-I.D. (0.515-inch-I.D.) glass tube, 109 cm (43 inches) long, with machined stainless-steel end fittings. Such a glass tube is rated to withstand an internal pressure of 500 psi, so the apparatus could be used to study priming with ammonia as the working fluid. Research in the present program was limited to methanol which is the working fluid in the heat pipes currently being built by TRW for spacecraft VCHP

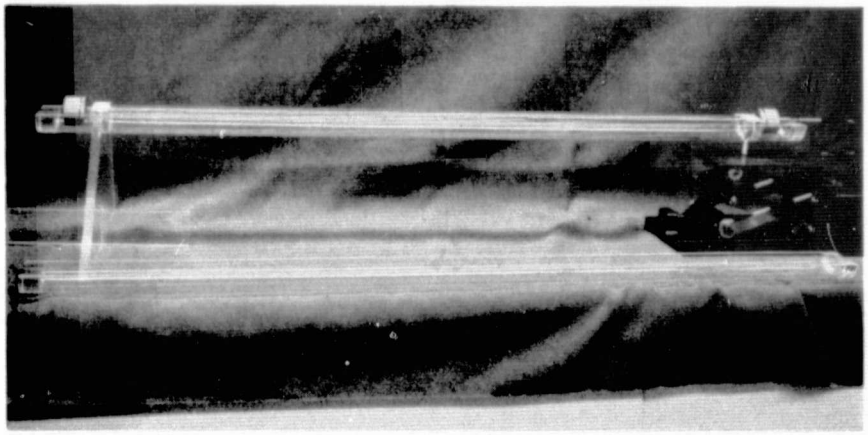

ORIGINAL PAGE IS
OF POOR QUALITY

Figure D-1. Glass Heat-Pipe Apparatus With Safety Shield Removed

applications. The glass pipe is held in a plexiglass cradle, which would also serve as a safety shield if ammonia were to be used.

The cross section of the heat pipe is shown in Figure D-2. The heat pipe is designed to closely model the two-artery/slab-wick heat pipes used in applications mentioned in the Introduction. The artery is spot welded to one side of the .127-cm-thick (0.050-inch-thick) felt-metal slab wick, and a .3175-cm-diameter (1/8-inch-diameter) sheathed rod heater with a 30.48-cm (12-inch) heated section is inserted into a double larger screen casing and is then spot-welded to the other side of the wick. The unheated end of the heater passes through and is brazed into the evaporator end cap. In the condenser region, a stainless-steel cooling loop extends along the opposite side of the wick as the artery. It passes through and is brazed into the condenser end cap. A .159-cm-diameter (1/16-inch-diameter) sheathed thermocouple extends into the adiabatic section so the vapor temperature can be monitored.

3. EXPERIMENTAL RESULTS

The experimental effort was first aimed at uncovering the cause of the discrepancy between computer predicted fluid charges and the larger charges actually required for the heat pipes to prime. As shown in Figure D-3(a), the foil-walled evaporator end of the artery (which we call a priming foil) has spiral rows of 0.0254-cm-diameter (0.010-inch-diameter) holes. The foil thickness is .00127-cm (0.0005 inch).

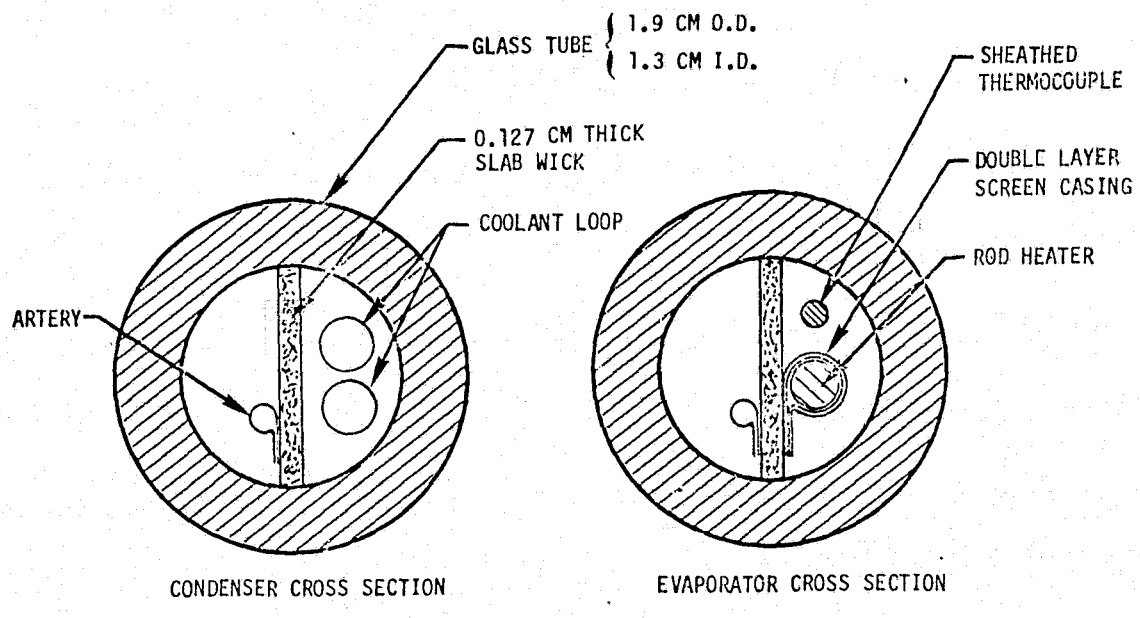

Figure D-2. Cross Section of the Glass Heat Pipe in the Condenser and Evaporator Regions

Priming tests consisted of first elevating the evaporator end of the glass heat pipe sufficiently so that the artery empties. A low heat load was applied. Then the evaporator end was lowered until the screen walled portion of the artery had filled with liquid. The elevation of the evaporator end relative to the condenser end was measured with a cathetometer. The evaporator end was lowered further until the foil-walled portion filled, and the evaporator elevation was measured again. Figure D-4 shows the results at several heat loads. The crucial finding is that the evaporator end must be depressed 0.25-cm to fill the priming foil after the screen-walled portion has primed. Previous computer predictions of required fluid inventories for priming, however, were based on the assumption that the screen-walled and foil-walled portion of artery have the same capillary pressure for priming. while the actual inside diameter of the foil region is 0.1854 cm (0.073 in.) the region behaves, as far as priming is concerned, as if its inside diameter were 0.244 cm (0.096 in.).

The reason for MULTIWICK underpredicting the fluid charges for priming is now clear. For example, the previously predicted minimum charge for the sounding-rocket heat pipes to prime was 17.9 cc of methanol, which was

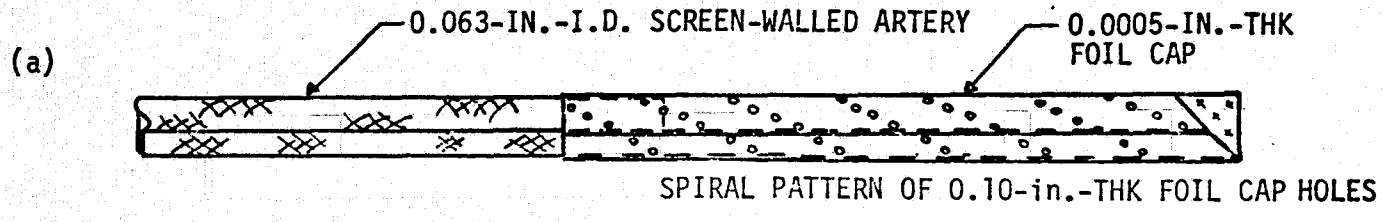

CTS PRIMING-FOIL DESIGN

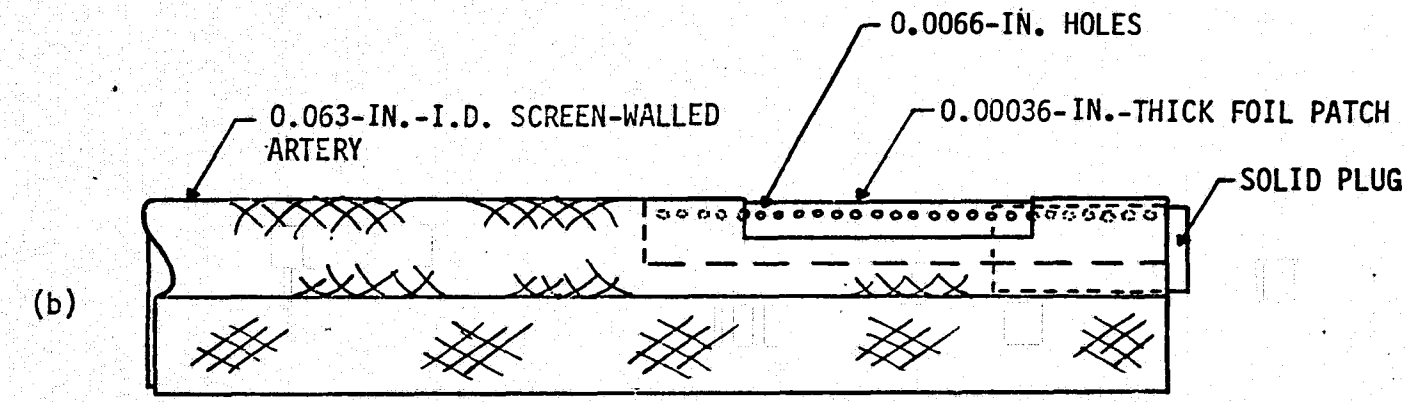

PATCH-OVER-WINDOW PRIMING FOIL

Figure D-3. Priming Foil Designs

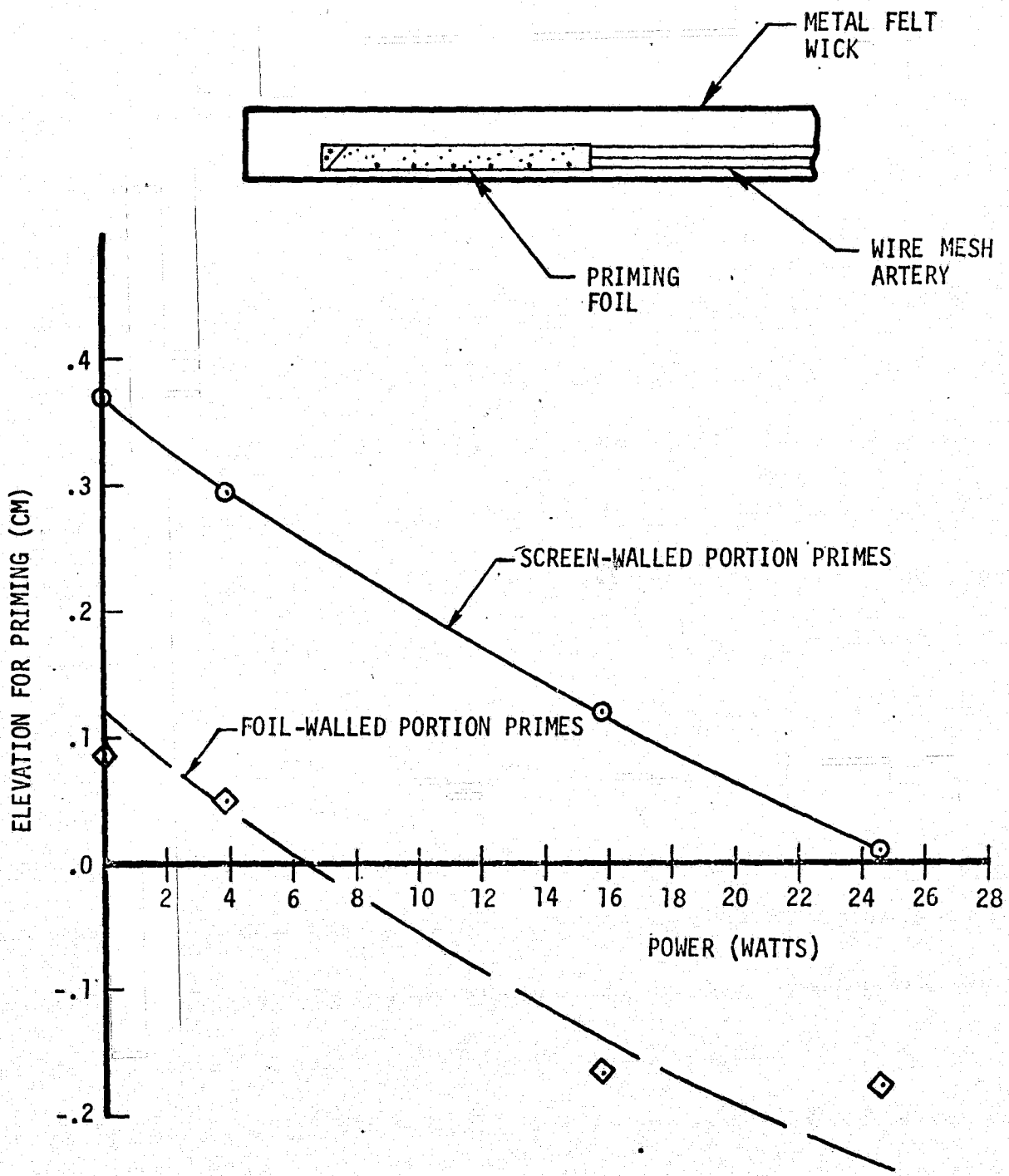

Figure D-4. Priming Characteristics of Artery With Priming Foil

based on priming the 0.160 cm (0.063-in.) - I.D. artery. MULTIWICK now predicts a minimum charge of 26.9 cc based on an effective inside diameter of 0.244 cm (0.096 in.) for the priming foil. The actual original charge of the heat pipes of 22.4 cc was, in fact, found to be insufficient for priming. When the charge was increased to 27.9 cc, the heat pipes primed reliably.

It was suspected that the reluctance of the priming foil to fill might be due to a finite non-zero wetting angle between the methanol and the foil. Oxidization is known to improve wetting especially with water. As an attempt to improve the priming performance, the wick and artery were removed from the glass heat pipe and oxidized by firing in air. As shown in Figure D-5, however, oxidization did not improve the performance.

It is now thought that the reluctance of the priming foil to fill is due to its slightly larger inside diameter of (0.073-in.) compared to the 0.160-cm-I.D. (0.063-in.-I.D.) of the main screen-walled portion and, more importantly, to the empty priming-foil holes pulling back by surface tension on the advancing meniscus as it crosses them. A new priming foil, shown in Figure 3(b), was designed to partially overcome these problems. The priming foil consists of a foil patch with a single row of holes, spot welded inside the screen-walled artery over a small window. The inside diameter of this design is essentially the same as that of the artery, and there is at most only one hole at any axial location along the priming foil to impede the advancing meniscus. Results of priming tests of this configuration, as displayed in Figure D-5, show that a hydrostatic head reduction necessary to fill the priming foil is 0.09 cm. This small reluctance to prime is desirable to ensure that the priming foil remains empty to vent gas until the entire screen-walled artery has primed. Although the actual inside diameter of the priming foil is that of the artery (0.160 cm or 0.063 in.), its effective inside diameter for priming is 0.183 cm (0.072 in.).

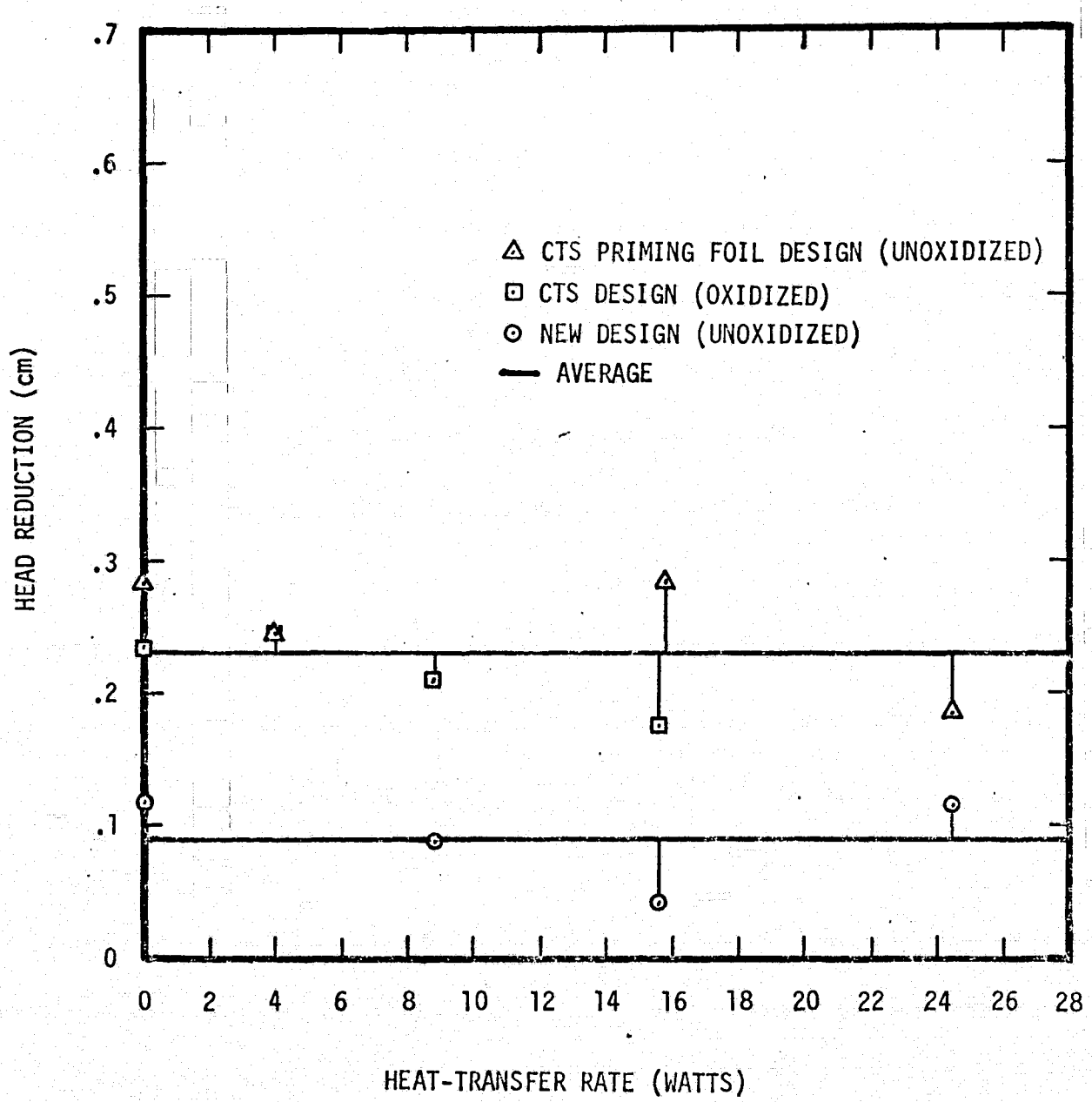

Figure D-5. Required Hydrostatic Head Reduction to Prime Foiled-Walled Region

In addition to having improved priming performance, the new priming foil was constructed of thinner foil (0.000914 cm or 0.00036 in.) that allows a smaller capillary hole size (0.0152 cm or 0.0066 in.). In comparison, the foils used for the sounding-rocket heat pipes were 0.00127 cm (0.0005 in.) thick with a capillary hole size of 0.0254 cm (0.010 in.). The small holes in the new design result in a 52% increase in heat-pipe capacity.

The next question investigated concerned convection of arterial bubbles. A bubble was trapped in the artery by raising the condenser end of the heat pipe high enough to empty the artery, and then leveling. The condenser end of the artery does not have a priming foil, and hence a bubble was trapped there.

A heat load was applied in attempt to convect the bubble to the evaporator end. Several runs were made for various heat loads and initial bubble sizes and locations. The results indicate that bubble convection was impossible at heat loads and evaporator elevations low enough for priming.

Bubbles were observed to convect at heat loads greater than for priming, however, when the bubbles entered the priming foil and vented, the artery would empty of liquid.

As a consequence of these results, for actual heat-pipe operation any arterial bubble that might exist would have to be cleared by applying a heat load in excess of the critical priming load, but below the maximum open-artery load. Then the load is reduced sufficient for priming. Another approach is to purposely ignore the existence of any arterial bubble. If a bubble did exist, a burnout would result the first time the heat load was increased above the open-artery capacity. Powering down below the critical priming load would result in successful priming because any bubbles would be convected to the evaporator end.

The next question investigated was concerned with the possibility of excess liquid flooding the venting holes of the priming foil. The evaporator end of the deprimed heat pipe was quickly dropped to level or even below level in attempt to trap a bubble by excess liquid submerging the priming foil. In every attempt, however, the artery completely primed before the venting holes were flooded. Failure to prime due to venting-hole flooding does not appear to be a problem.

4. CONCLUSIONS

The glass heat pipe has been a powerful tool in furthering our understanding at priming principles. The current research effort for a methanol, slab-wick, priming-foil/artery heat pipe has shown that:

- The priming-foil design used for the sounding-rocket experiment (and CTS) primes as if its I.D. were 0.244 cm (0.096 in.) instead of its actual I.D. of 0.185 cm (0.073 in.).
- The larger effective I.D. explains the required fluid charge for priming being significantly larger than previously predicted.
- The large effective I.D. is due to holes in the priming foil imposing a surface-tension retarding force on the advancing meniscus.
- By placing the priming foil with a single row of holes inside a "window" in the artery, the priming foil effective I.D. is reduced to 0.183 cm (0.072 in.), which is only slightly larger than the artery I.D.
- To clear an arterial bubble that has somehow been trapped somewhere along the artery other than in the priming foil, a heat load in excess of the critical priming load is required.
- Excess liquid could not block the priming-foil holes to prevent venting - venting always occurred before the holes were flooded.